S
U

Universitetet
i Stavanger

FACULTY OF SCIENCE AND TECHNOLOGY

MASTER'S THESIS

Study programme/specialisation: Marine and Offshore Technology	Spring semester, 2019 Open
Author: Denis Shatilov	*[signature]* (signature of author)
Supervisors: Daniel Karunakaran (Subsea 7), Peter Orimolade (Subsea 7), Ove Tobias Gudmestad (UiS), Alexander Ivanovich Ermakov (Gubkin University)	
Title of master's thesis: Design features of offshore facilities for South-Western Kara Sea conditions	
Credits: 30 ECTS	
Keywords: Kara Sea, South-Western part, Pipeline system, S-Lay, Pipeline route, On-bottom stability, Passive resistance, Curved laid method, SIMLA, Arctic region, Offshore structures, GBS, Topside, Icebergs, Ice conditions, Pobeda field, Conditions of natural environment.	Number of pages: 88 + supplemental material/other: 2 Stavanger, June 15, 2019

Title page for Master's Thesis Faculty of Science and Technology

Abstract

The increasing hydrocarbon deposit depletion degree leads to the necessity to engage new promising territories in field development. In Russia, the depletion of petroleum fields has exceeded 50% of their potential, while even the maximum field development of explored reserves will not be able to give the required hydrocarbon production level. According to the research estimation (Zolotukhin, 2019), 93% of hydrocarbons accounted for in the Arctic region are concentrated in a dozen of large fields. The percentage of gas in Arctic hydrocarbon reserves reaches 78% while the percentage of oil is 22%. Moreover, two thirds of petroleum fields are located on Russian territory.

The Kara Sea is a part of the Arctic shelf and it has significant hydrocarbon reserves. Pobeda is one of petroleum deposits situated on Kara Sea shelf. In the Arctic harsh conditions, careful analysis is required for the effective field development of this field. Eventually, it is necessary to apply robust technologies and concepts for Arctic offshore fields, including the Pobeda field. In frame of the master thesis, technological evaluation (namely, technological readiness and risk evaluation) will be discussed. There are two major areas for evaluation. They are offshore construction and offshore transportation system. The first part emphasizes the proper selection of offshore structure, discussing previous experience of arctic field development and analyzing platform design with software and appropriate calculations. The second part considers the hydrocarbon transportation system paying much attention to pipeline design/installation. Pipeline route, pipeline design and installation method will be discussed in this section. For the issues of pipeline routing, the SIMLA software is used.

The final chapter of the master thesis gives a technological evaluation and discusses economic aspects for the Pobeda field development. Risk matrix and analyses are included and future recommendations with conclusions are given. The Master thesis suggests conceptual designs, consequently different assumptions are proposed.

Acknowledgements

Content

List of figures

List of tables

List of symbols

b - Pipe buoyancy per unit length

d - Water depth.

D - Pipe outer diameter including all coating

E – Young modulus

F_Y - Horizontal hydrodynamic (drag and inertia) load

F_Z - Vertical hydrodynamic (lift) load.

F_R - Passive soil resistance

F_C - Vertical contact force between pipe and soil

g - Acceleration of gravity.

G_c - Soil (clay) strength parameter

H – Horizontal bottom tension

Hs - Significant wave height during a sea state.

k_T - Ratio between period of single design oscillation and design spectrum .

k_U - Ratio between oscillatory velocity amplitude of single design oscillation and design spectrum .

K - Significant Keulegan-Carpenter number

M - Steady to oscillatory velocity ratio for design spectrum

M^* - Steady to oscillatory velocity ratio for single design oscillation V^* /U^*.

r_{tot} - Load reduction factor.

r_{tot} - Load reduction factor due to penetration.

r_{tr} -Load reduction factor due to trench.

r_{perm} -Load reduction factor due to a permeable seabed.

R_D - Reduction factor due to spectral directionality and spreading.

R_C – Curved radius

s_g - Pipe specific density .

s_u - Un-drained clay shear strength.

T_u - Spectrally derived mean zero up-crossing period

T_p - Peak period for design spectrum.

T_n - Reference period

T^* - Period associated with single design oscillation.

U_W - Wave induced water particle velocity.

U_S - Spectrally derived oscillatory velocity (significant amplitude) for design spectrum, perpendicular to pipeline.

U^* - Oscillatory velocity amplitude for single design oscillation, perpendicular to pipeline.

V^* - Steady current velocity associated with design oscillation, perpendicular to pipeline.

w_d - Pipe dry weight per unit length.

w_s - Pipe submerged weight per unit length.

z - Elevation above sea bed.

z_r - Reference measurement height over sea bed.

z_0 - Bottom roughness parameter

z_p - Penetration depth.

α – thermal expansion coefficient

ρ_w – mass density of water

ρ_s – mass density of steel

ρ_p – mass density of anticorrosion protection

ρ_c – mass density of concrete coating

η_l – safety factor

σ_e – equivalent stress

σ_h – hoop stress

σ_l – longitudinal stress

υ – Poisson ratio

μ_s – friction coefficient of soil

γ_W – safety coefficient

Introduction

State of art

For decades, the major sector in Russia for hydrocarbon production was the West Siberian region, which comprises huge onshore fields. They contain enormous quantities of hydrocarbons with peak production rates taking place in the end of 1980's (Heinkel, 1997).

As operated oil and gas fields are depleting, for the petroleum industry there is an issue to search new hydrocarbon resources in offshore areas. Due to this cause, the Arctic shelf importance grows up every year and it is proposed to be a major object for future developments. Initial estimations show that Russia possesses incredible reserves of oil and gas in the Arctic region. These reserves are equal to 100 billion tons of oil equivalents. However, field development concepts require accurate consideration and thorough analysis due to harsh environmental conditions.

Pobeda oil/gas field is located in the southwestern part of the Kara Sea (Figure 1). This field is located on the license area of East-Prinovozemelsky-1 (EPNZ-1). It is situated 250 kilometers from the mainland of the Russian Federation. A total recoverable reserve reaches 130 million tons of oil and 499 billion cubic meters of gas (Rosneft presentation, 2017). For proper and stable field development and its future exploitation, it is necessary to choose appropriate marine offshore structure and hydrocarbon transportation system and to perform technological evaluation for chosen objects for Pobeda oil/gas field. Technological evaluation will be based on technological readiness and possible risks. Afterwards, there will be some economic aspects regarding to Pobeda field development.

Figure 1 – Pobeda field location (Rosneft, 2017)

The scope of work

The aim of this master thesis is to give technical evaluation after selecting the appropriate marine offshore structure according to natural conditions and analyzing pipeline route between field and onshore infrastructure. These are the main steps:

- Describe the environment characteristics of the Kara Sea at Pobeda field area;
- Propose the appropriate type of offshore structure according to ice cover impact;
- Suggest types of hydrocarbon transportation for given natural conditions;
- Describe the design criteria of pipeline and its installation method;
- Check lateral on-bottom stability of pipeline which is laid along a curved method using SIMLA software;
- Present technical evaluation and economic aspects for given objects.

Previous works

There are a lot of articles, reports and papers (some of these will be referenced later) about the field development in the Arctic shelf. Moreover, similar field development concepts were applied for existing field with familiar natural conditions. There are some patents and research works, which are intended to make robust and stable infrastructure for Arctic shelf for sufficient hydrocarbon extraction.

Chapter 1. Natural conditions at the Pobeda field

Climate conditions

The climate is cold and marine. The winter is long and cold in the Kara Sea. In the summer, cool cloudy weather prevails with light winds mainly from the north. In the autumn, the wind speed increases. The southwestern part of the sea has a milder climate than its northeastern part.

Thermal regime

The features of the Kara sea geographical location and the atmospheric circulation above the sea create distinct differences in the thermal regime over different parts of the sea. The average annual temperature is 5–7°C higher over the southwestern part than over the northeastern one. In the southwestern part the coldest month is February, the warmest month is August. The January average temperature of the sea is –21°C in the southwestern part. In July, the air temperature is above 0°C practically over the Kara Sea entire water area. Average temperature values fall below 0°C in the southwestern part in late September and early October. This late transition to sub-zero temperatures is associated not only with the advection of the warm air in cyclones, but also with the thermal effect of water masses coming to the Kara Sea from the Barents Sea (AARI, 2017).

Atmospheric pressure

According to the data of the Russian Arctic sea island hydrometeorological stations, the annual atmospheric pressure trend at the sea level for EPNZ area is presented in Table 1.

Table 1– Monthly average atmospheric pressure at the sea level, GPa (Gabdullin, 2014)

Kara sea, East-Prinovozemelsky area												
I	II	III	IV	V	VI	VII	VIII	IX	X	XI	XII	Year
1008	1011	1010	1009	1007	1011	1012	1011	1009	1007	1012	1012	1010

Wind

The wind conditions over the Kara Sea are characterized by large interannual variability. Thus, in some winters, the northeastern wind was the predominant wind, and sometimes in the summer season, western air heatwave prevails and causes wind waves on the surface of the water. Average wind speeds over the Kara Sea vary slightly from season to season, and the annual amplitude does not exceed 1 - 3 m/s. The highest average values associated with increased cyclonic activity during this period (8 m/s) are observed in autumn and winter. In summer, the wind speed drops to 5 m/s. Wind speed depends on its direction; usually the strongest winds are from the western direction.

In the coastal region of the southern part of the sea, the highest speeds are observed in the

south winds. In the southwestern part, there are moderate wind speeds. A local hurricane wind often forms Novaya Zemlya bora along the shores of Novaya Zemlya. It usually lasts several hours, but in winter, it can last up to 2–3 days. The highest wind speeds are presented in Table 2.

Table 2 – Monthly maximum wind speed at gusts for East-Prinovozemelsky area, m/s (Gabdullin, 2014)

Kara sea, East-Prinovozemelsky area											
I	II	III	IV	V	VI	VII	VIII	IX	X	XI	XII
25	40	30	25	25	40	26	30	34	40	34	40

The icing-up of surface objects

For the shelf zone of the Arctic seas, there is a significant recurrence of hydrometeorological conditions under which the icing-up of surface objects occurs, including vessels and offshore structures. Under natural conditions, there are three types of icing-up:

1. Sea icing-up. It is the freezing of ice on objects due to splashing and flooding with sea water;
2. Atmospheric icing-up. It is the deposition of ice on the surface of objects, due to the sublimation of steam, as well as the freezing of raindrops, drizzle, sleet, fog;
3. Mixed icing-up. It is the freezing of precipitated snow moistened with seawater, as well as a combination of the first two types of icing-up.

The negative air temperature in the Kara Sea is observed in any months of the year, so atmospheric icing-up of the surface object is possible here at any time of the year. As the sea surface is cleared of ice, conditions rise which are favorable for the development of waves in the sea, and, therefore, splashing and flooding of the object and its icing-up. In the southwestern part of Kara Sea, this is observed from July to October. Particularly, intensive icing-up of vessels is observed in September and October. At the same time, all three types of icing-up are possible. In accordance with the statistical processing of vessel observations in the Arctic seas for the period from July to September since 1955 to 1982, sea icing-up is observed on average in 50% of cases, mixed one is observed in 41% of cases and atmospheric one is observed in 9% of cases. There are three kinds of icing-up depending on icing-up speed (AARI, 2006):

1. Slow icing-up occurs at air temperature from 0 to -3°C and any wind speed, as well as at air temperature below -3°C and wind speed up to 7 m/s;
2. Rapid icing-up occurs at air temperatures from -4 to -8°C and wind speed of 7-15 m/s;
3. Very rapid icing-up is observed at air temperatures below -3°C and wind speeds of more than 15 m / s, as well as at air temperatures below -8°C and wind speeds of more than 7 m / s.

In the Kara Sea in the first half of navigation (July-August), the hydrometeorological conditions on the navigable sections of the route do not contribute to the development of rapid and very rapid sea. During this period, the slow freezing of surface objects is possible, the probability of which increases from 1-5% in the southern part of the sea. In the second half of navigation (September-October) all three degrees of sea icing-up are noted. In September, the probability of slow icing-up ranges from 20% in the south of the sea to 70% in the north, the probability of rapid icing-up is up to 10% and the probability of very rapid icing-up is up to 5% in the north of the sea. In October, the probability of a combination of negative air temperature and strong winds increases, so the probability of all degrees of icing-up increases on the air highways in the sea. During this period, the probability of very rapid icing-up increases from 2-10% in the first decade to 10-30% in the third decade.

The average duration of ice buildup during sea icing-up does not exceed 2-3 days, and the longest one lasts 7 days. There were cases in which 20-40 cm ice thick had been deposited on the ship's deck during the period of sea icing-up. Statistical processing of observations of atmospheric icing-up on the ice machine at polar stations showed that the most frequent type of atmospheric icing-up in the Kara Sea is crystalline hoarfrost (68% of all cases of atmospheric icing-up) and icy spots (25% of cases). Grainy hoarfrost occurs less frequently (6% of cases). The deposits of wet snow and complex atmospheric icing-up (several types of atmospheric icing-up at the same time) are rarely observed (less than 10% of cases). A brief description of various types of atmospheric icing-up is below (AARI, 2006).

Crystalline hoarfrost is deposited by the sublimation of steam on thin objects in the form of ice crystals of leaf-like shape. It is most often (90% of cases of crystalline hoarfrost) formed at air temperatures from -8 to -38°C and low wind (0-4 m/s). Greatly less (10% of cases) the deposition of frost is observed at air temperatures below -40°C. In winter, these deposits can persist for one to two months, and in spring and autumn their duration lasts from several hours to several days. The period of crystalline hoarfrost rise usually does not exceed 1-2 days. Most often (80% of cases) the thickness of ice deposits does not exceed 1 cm, less often the thickness is 2 cm and only in some cases it is more than 5 cm. The maximum thickness of hoarfrost deposits in the Kara Sea does not exceed 20 cm (Gabdullin, 2014).

Granular hoarfrost forms when mist droplets freeze when air temperature varies from -2 to -18°C and light wind (less than 4 m/s). Separate cases of this type of icing-up were also recorded at air temperature of about -40°C and strong wind. Unlike crystalline hoarfrost, the granular one is a dense snowy ice cover, having a density of 100-500 kg/m^3. The period of granular hoarfrost rise does not exceed 2-3 days. The thickness of the deposits is usually small (0.5-1.0 cm) and in rare cases reaches 5 cm. Granular hoarfrost persists for 1–3 days, and in the

north of the Kara Sea the process of destruction can last up to 10 days.

Icy spots are formed when freezing raindrops or drizzle at air temperature from 0 to -1°C and wind speed of 0-12 m/s. During one day the ice crust increases to 1-2 cm and only in some cases it achieves up to 5-6 cm. Normally, icy spots and granular hoarfrost are observed in spring and autumn, while crystalline hoarfrost occurs more often in winter.

The deposition of wet snow is observed at an air temperature of about 0°C and a wind speed of 5 to 15 m/s. Often the deposition of wet snow is accompanied by the formation of icy spots. The wet snow deposition density values range from 300 to 600 kg/m^3. The thickness of deposits in most cases (more than 90%) does not exceed 1 cm and only in some cases it reaches 2 cm. The deposits of wet snow are unstable and usually collapse during the day. In some cases, the formation of alternating layers of crystalline hoarfrost, icy spots and granular hoarfrost on the surface object is observed. With this type of icing-up, the thickness of ice deposits is 1-2 cm, and the weight is 150 g (AARI, 2017).

Atmospheric icing-up complicates the work of locators, radio antennas, and in some cases leads to an emergency. The obtained characteristics of atmospheric icing-up are sufficiently representative for the sea area, since all the stations whose observations were used are located at a small height and near the coastline. In addition, for most of the year, the underlying surface, both at sea and on land, is homogeneous (snow cover). Often in the Kara Sea, atmospheric icing-up and sea icing-up occur simultaneously. Often times, this occurs when the snow falls in strong wind and frost. As a result, the surface of overwater objects is covered with ice, the density of which is 500-700 kg/m^3. With mixed icing-up, the maximum thickness of the ice layer, which freezes on the deck of the vessel, can reach 100 cm, and on hydraulic structures it can be two times more (Gabdullin, 2014).

Hydrological conditions

Water temperature

The waters of the Kara Sea warm slightly, consequently they have low temperature. In the surface layer, the temperature decreases from southwest to northeast. In the autumn-winter period, the surface is strongly cooled, and in ice-free water, temperature quickly drops. In winter, in the under-ice layer of water, the temperature is everywhere close to the freezing point at a given salinity. In the southern part of the sea, which is first released from ice and is influenced by river flow, the water temperature gradually increases. During the warmest summer months, the water temperature reaches +3–6°C, and in ice-covered areas it slightly exceeds the freezing temperature at a given salinity.

The temperature of the water in the Kara Sea in winter from the surface to the bottom

practically does not change. An exception is St. Anne Trough and Voronin Trough, through which warm saline Atlantic waters flow into the Kara Sea. Here, in the depth range from 50 to 300 m, positive values of water temperature are noted. In spring, on ice-free areas in the south, radiation heating spreads from the surface depthward. Water temperature above 0°C is observed to depths of 15–18 m in the southwestern part of the sea and to depths of 10–12 m in the southeastern one. Thus, the deeper the water the temperature drops sharply. In the northern part of the sea, where there is ice cover, the winter temperature distribution of water is maintained vertically. In the warmest months in the shallow parts of the Kara Sea, the water temperature is positive from the surface to the bottom. In the western part of the sea, a relatively high temperature of water is observed to a depth of 60–70 m, in the eastern part, water temperature on the surface has positive values, but it decreases to negative quickly to the bottom, close to the freezing temperature at a given salinity. At the beginning of the autumn cooling, the temperature of the water on the surface is slightly lower than in the subsurface layers. Autumn cooling levels the temperature throughout the water column, with the exception of areas where Atlantic waters are distributed (Gabdullin, 2014). The average monthly water temperature in the surface layer for East-Prinovozemelsky area is given in table 3.

Table 3 – Monthly average water temperature in the surface layer, °C (Gabdullin, 2014)

Kara sea, East-Prinovozemelsky area												
I	II	III	IV	V	VI	VII	VIII	IX	X	XI	XII	Year
-1,7	-1,7	-1,1	-0,5	-1	2	3	2	1	-0,5	-1,2	-1,8	-0,2

The Kara Sea is widely open to the Arctic Basin of the Arctic Ocean, which determines its hydrological regime, in addition, the continental runoff of the large rivers (Ob, Yenisei, and others), which accounts for 55% of the total river flow to all the Arctic seas. Continental waters, creating a surface desalination layer, influence almost 40% of the sea area. The surface layer in July after thawing of the ice quickly warms up to an average of 3°C. In August, its temperature may reach a maximum of 10°C. There is no effective mixing of water vertically. In the near-surface layer, a stable layer of an abrupt temperature change along the vertical is formed. This is a thermocline, which is most pronounced in August-September, extending from the surface to a depth of 20-30m. The deeper the water, the temperature remains almost uniform and does not exceed an average of 0,5°C, dropping to 0°C at the bottom. In October, the average monthly temperature in the surface layer decreases to 1°C, the thermocline disappears, the temperature is about the same throughout the entire thickness of the seawaters (AARI, 2017).

The salinity of the Kara Sea is influenced by water exchange with the Arctic basin, large continental runoff, and ice melting and ice formation. The salinity of the surface waters of the

sea varies from 3–5‰ in the south to 33–34‰ in the north. In the cold season, when ice formation occurs and the continental runoff is minimal, the salinity increases and it is 25–30‰ with the exception of the estuarine areas.

Since July, in the surface layer of the sea, because of ice melting, the salinity of water decreases, and a halocline is formed. Halocline is a layer of abrupt salinity variation vertically. During the summer, its lower boundary is located at a depth of about 20-30m. Below, the salinity varies little (Gabdullin, 2014).

In accordance with the temperature distribution and salinity in the upper 20-30 m layer, a stable layer of a seawater density jump (seasonal pycnocline) is formed with a sharp increase in density with depth. Pycnocline is most clearly expressed in August, during the maximum warming up of the water surface and the maximum distribution of fresh river water. The influx of river waters in spring, their distribution in the water area and the melting of ice reduce the salinity of the surface layer in the summer. Salinity increases from the surface to the bottom of the sea. In winter, in most parts of the sea, the salinity evenly increases from 30‰ on the surface to 35‰ at the bottom.

Dissolved oxygen

A striking feature of the seasonal pycnocline of the southwestern part of the Kara Sea is the layer with the maximum oxygen concentration. Maximum values are observed at a depth of 10–15 m. The subsurface maximum of the oxygen content is observed not only in the South-West part, but also in the Northern part of the Kara Sea. In the main pycnocline in the southwestern part of the Kara Sea, the oxygen concentration decreases sharply. In the deep layers of the Novaya Zemlya depression, it is often below 6.0 ml/l. A special feature of the vertical structure is the warm Atlantic water masses with high oxygen content, coming from the Arctic basin in the St. Anne Trough and Voronin Through. The amount of oxygen on the bottom horizons is usually from 6.7 to 6.9 ml/l (Gabdullin, 2014).

Tidal phenomena

In the Kara Sea, tidal wave comes from the west from the Norwegian Sea. The tides are expressed in the Kara Sea very clearly. One tidal wave comes from the Barents Sea and spreads to the south along the east coast of Novaya Zemlya, the other tidal wave goes from the Arctic Ocean to the south along the western shores of Northern Earth. When approaching the shores, the waves are reflected from them, interfere and change their height. All this complicates the picture of tides in the Kara Sea, where correct semi-diurnal tides mostly prevail, but diurnal and mixed tides are observed in some areas. Tidal level changes are relatively small. On all points of the coast, they are on average 0,5–0,8m, but they exceed 1m in the Ob Bay. Frequently, they are obscured by surges, which are more than 1m on the continental coast of the sea, and in the depths

of bays in iceless seasons, it reaches 2m and more. Table 4 gives information about the characteristic of the level mode at the Pobeda field area.

Table 4 – The characteristic of the level mode at the Pobeda field area (Gabdullin, 2014)

Characteristic	Mark relative to the sea level recorder, centimeters
Maximum measured level	86,6
Maximum upsurge	65,4
The highest possible astronomical conditions (HAT)	55,4
Mean Sea Level (MSL)	0
Maximum negative surge	-39,3
The lowest possible astronomical conditions (LAT)	-60,8

Tidal level fluctuations are correct semi-diurnal. In total sea level fluctuations, the contribution of tidal phenomena is about 67% of the total dispersion of sea level fluctuations.

Sea level

In areas of the Kara Sea, where the influence of river flow is relatively small, there is a sharp increase in maximum levels in September and maintains their increased background until March. In April, the values of maximum sea levels sharply decrease and remain relatively low until August.

Such a nature of seasonal sea level variability corresponds to the intensification of cyclonic activity over the Kara Sea.

Currents

The characteristics of the Kara seawater circulation are determined by the huge river flow of the Ob and Yenisei rivers, which form a positive level anomaly in the mouth area (Figure 2).

As a result, the current from the Ob Bay spreads partly to the west along the periphery of the dome of freshened waters, and not to the east, as it is typical for river waters in the northern hemisphere. In the central part of the sea, the current is divided into two branches, one of which goes to the Central Arctic Basin along the St. Anne Trough and Voronin Trough, the other one goes to the Laptev Sea through the Vilkitsky Strait and Shokalsky Strait.

The Barents Sea waters flowing through the Kara Strait are transported across the sea along the eastern slope of the Novaya Zemlya Basin.

The average velocity of constant currents in the area of the field varies from 5 to 15 cm/s, the predominant direction is south-west, although the main flow does not have a robust direction. Its direction on the surface may be disturbed by local vortex formations and changed under the action of the wind. The registered current velocities in the surface layer at the Pobeda field are more than 1 m/s, and current velocities in the layer of 20-25 m are equal 0.85 m/s. Table 5

presents current velocities at 40m water depth (AARI, 2006).

Table 5 – Current velocities at Pobeda field area (Gabdullin, 2014)

Characteristic	Average value	Maximum	Repeatability period, years		
			5	10	100
Level 40-meter depth					
All directions	7	54	42± 9	45±10	57±21
N	6	49	36±15	41±17	57±21
NE	7	49	38±10	42±12	53±15
E	7	40	33± 8	36±10	45±12
SE	9	53	42± 9	45±10	55±13
S	8	54	40±11	44±13	56±16
SW	6	41	34±10	37±11	48±14
W	4	24	20± 6	22± 7	29± 9
NW	4	41	28±12	33±14	46±18
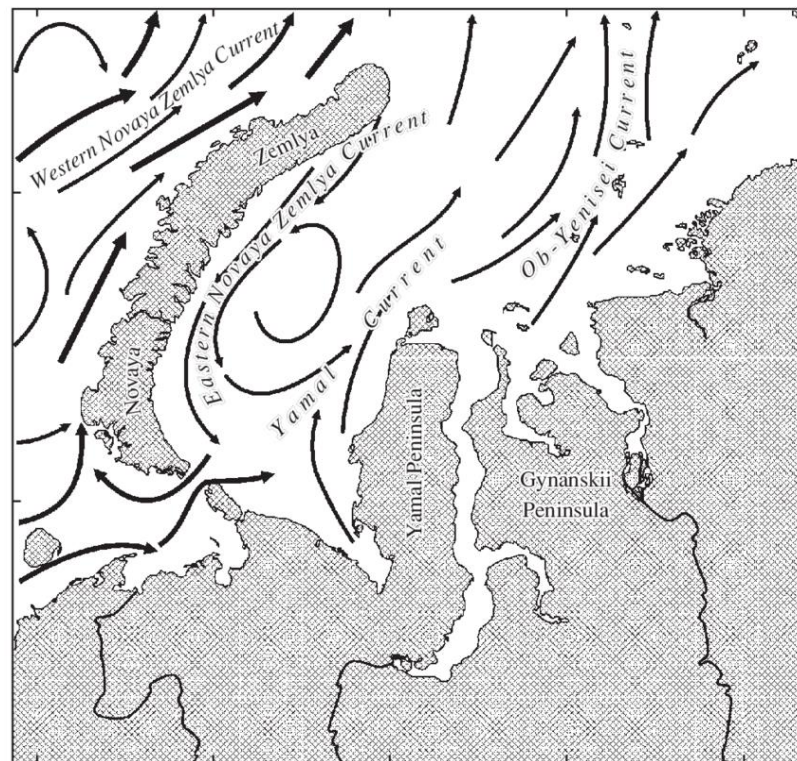
Figure 2 – Kara sea current scheme (Galimov et al., 2006)

Wind-driven wave

Frequent and strong winds cause significant waves in the Kara Sea. However, in addition to the speed and duration of the wind, wave heights depend on the sea ice extent affecting the length of the wind acceleration. In accordance with this, the strongest excitement is observed in the little icy years at the end of summer or the beginning of autumn. Waves with a height of 1.5–2.5m have the highest repeatability; waves with a height of 3m and more are less often observed; the maximum wave height can exceed 8m. Strong wind waves develop in the southwestern and

northwestern parts of the sea, which are usually free from ice. The central shallow-water areas of the sea are characterized by weaker wave development. (Gabdullin, 2014). Table 6 shows the extreme values of wave heights of different exceedance at Pobeda field.

Table 6 - Estimates of the extreme values of wave heights of different exceedance in Pobeda field area (Gabdullin, 2014)

Characteristic	Period of repeatability, years		
	1	10	100
Average wave height, m	2,9	3,9	5,1
Significant wave height hs, м	4,7	6,2	8,2
Wave height 3% exceedance h3%, м	6,1	8,1	10,2
Wave height 1% exceedance h1%, м	7,0	9,3	12,2
Wave height 0.1% exceedance h0,1%, м	8,5	11,3	14,9

Ice conditions

Ice formation

The most important in the annual cycle of changes in ice conditions in the Arctic seas is the autumn-winter period (from October to May), during which the formation and growth of ice occur and it creates conditions for the steady accumulation of ice (Figure 3). The time of sustainable ice formation is one of the main characteristics, which largely determines the complexity of ice conditions in the winter period. Most often, severe ice conditions (increased thicknesses and an unfavorable distribution of ice) are formed following the early periods of sustainable ice formation. Depending on the changes in hydrometeorological conditions at all stages of the development of ice cover, ice characteristics may differ significantly from the average values, that determines the range of changes in ice conditions in the Arctic seas from light condition to heavy one. On average, ice formation begins among cohesive ice on the northern borders of the Arctic seas in late August and early September, then it spreads to areas of rarefied and rare ice, after which it covers pure water zones with increasing ice thickness. Shore fast ice is formed in the coastal shallow areas. During this period, all the seas of the Siberian shelf are completely covered by ice of various ages (thickness) with coverage of 9–10 points.

In the Kara Sea ice formation begins in late August and early September in the northeast of the water area, mainly among the residual ice, and this process usually lasts during two and a half months. During the second half of September, ice formation spreads along Severnaya Zemlya Island and the Taimyr Peninsula, as well as in the Vilkitsky Strait.

In the first decade of October, initial types of ice are observed in the entire water area of the northeastern part of the sea. Then freezing gradually spreads to the southwestern part, where it usually begins in the freshened waters of the Ob – Yenisei coast, as well as near the northern Novaya Zemlya Island. During October and the first half of November, the "trend" of ice

formation spreads to most of the coastal and open areas of the southwestern part of the sea, and in the third part of November, the primary forms of ice appear in the Kara Strait.

After freezing, the thickness of the ice gradually increases, reaching a maximum by the end of the cold period (May). In the southwestern part of the sea, by the end of the ice cover period, a large part of the sea area is occupied by one-year thick ice (more than 120 cm thick). At the same time, in the north of the water area, their thickness is about 140-160 cm, in the south part it is about 120-140 cm (AARI, 2017).
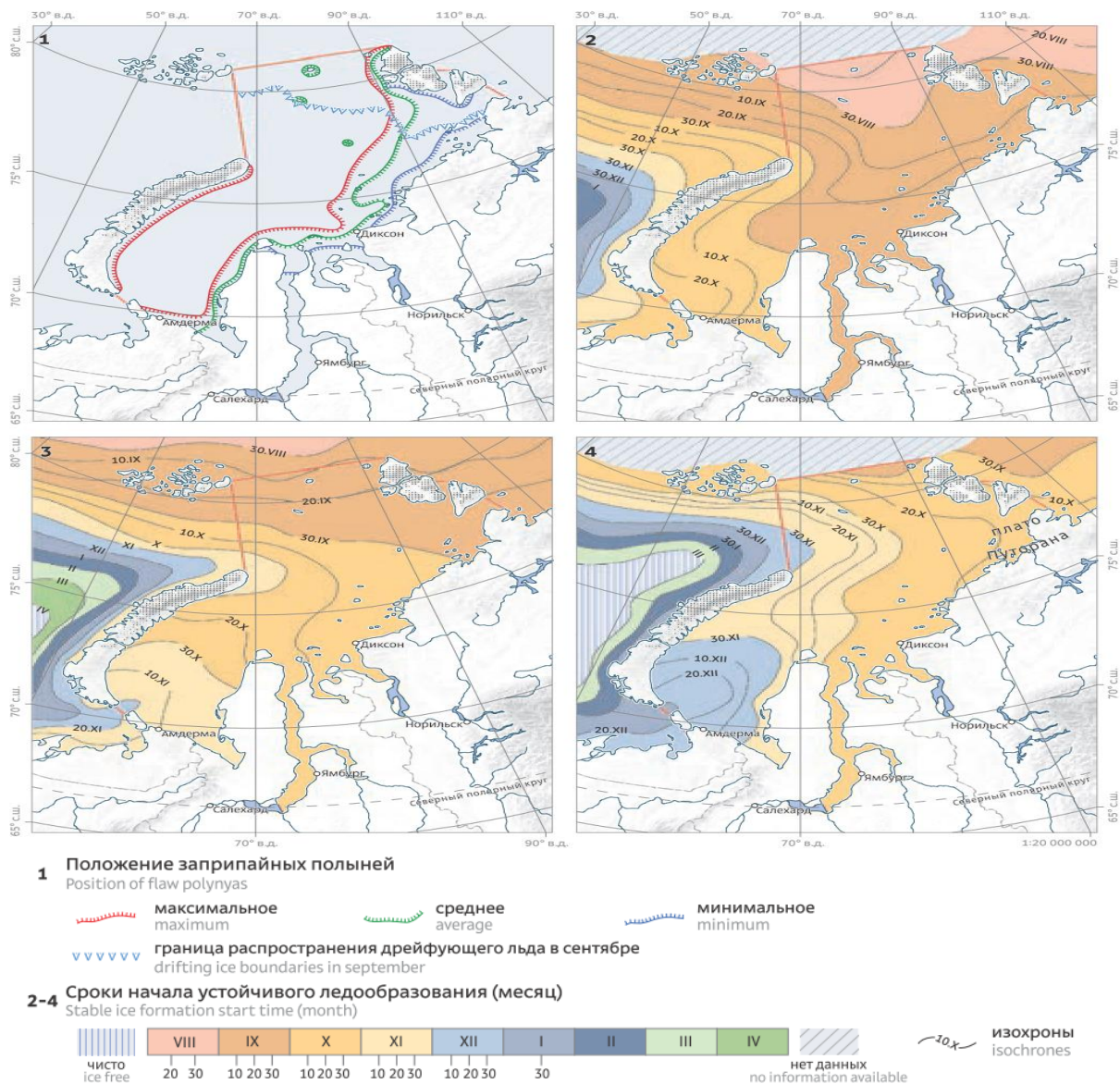
Figure 3 - Ice situation and the time of ice formation (Gabdullin, 2014)

Shore fast ice

The shore fast ice forms soon after a steady ice formation and is formed until March-April, after which its boundary stabilizes. At the end of the growth period, shore fast ice occupies from 20 to 33% of the total ice cover of the Arctic seas of the Siberian shelf.

The main areas of shore fast ice formation are associated with shallow and insular areas. These conditions are fully consistent with the northeastern part of the Kara Sea. Shore fast ice is less developed in the southwestern parts of the Kara Sea and Chukchi Sea, where its maximum width does not exceed 200 km. In the southwestern part of the Kara Sea, the shore fast ice thickness is 150–160 cm in average.

Flaw polynya

With almost constant removal of ice from the sea to the north in winter, large areas of flaw polynyas and young ice remain outside the shore fast ice (Figure 4). The width of this zone varies from tens to several hundred kilometers. Its separate sections are called the East-North-Zemlya, Taimyr, Lensk and Novosibirsk polynyas. At the beginning of the warm season, the last two polynyas reach enormous sizes (thousands of square kilometers) and become centers of the sea cleansing from ice. Melting of ice begins in June - July and significant sea areas are free from ice by August. In summer, the ice edge often changes its position under the influence of winds and currents. In general, the western part of the sea is icier than the eastern one. From the north, along the eastern coast of Taimyr, the spur (edge) of the oceanic Taimyr ice massif descends into the sea. This spur often contains heavy perennial ice. It persists until new-year formation, depending on the prevailing winds, moving to the north, then to the south. Flaw polynyas are formed along the entire boundary of the shore fast ice of the Arctic seas (AARI, 2017).
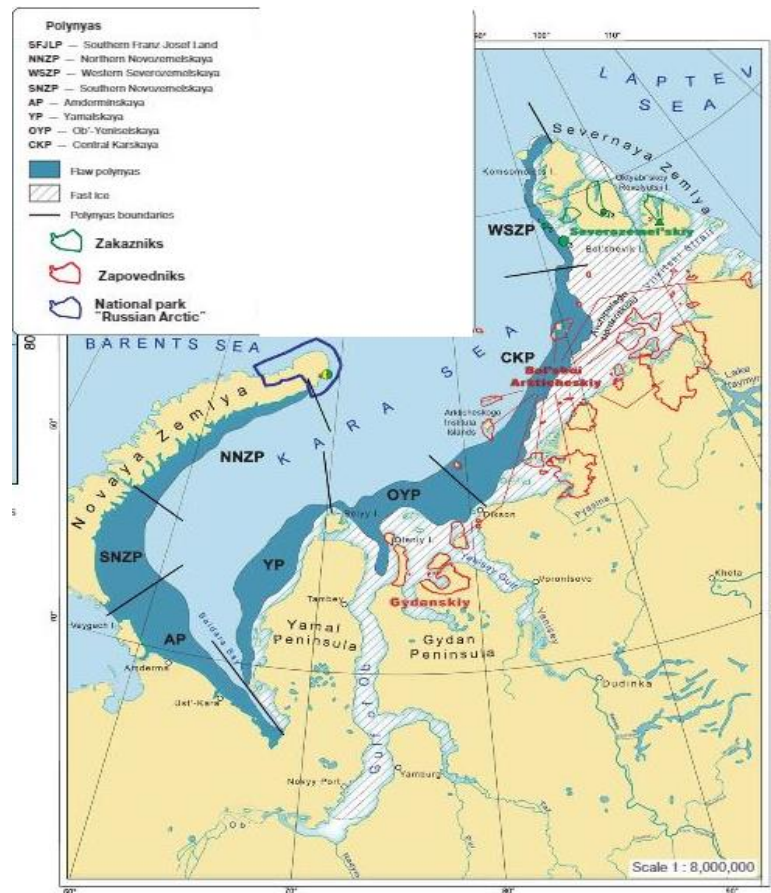
Figure 4 – The flaw polynyas of Kara sea (Spiridonov et al., 2011)

Ice hummocks

Hummocking is very characteristic of the ice cover of the polar and freezing seas. There are three types of hummocking:

1. Wind hummocking. It is the most powerful that occurs when pressure winds;
2. Tidal hummocking. It occurs due to inhomogeneous changing speed at a short distance and direction of tidal currents;
3. Thermal hummocking, which is the weakest of above-mentioned.

In the Arctic seas, ice hummocks predominate in the shape of ridges. They are represented as the conglomeration of ice fragments stretched in a certain direction, which can extend to distances from tens to hundreds of meters. The height of the hummock ridges can reach 5-6m, and the draft of the keel might be 20-25m. In the Kara Sea, ridging hummocking composes 1–2 points (10 to 20%) on most part of the shore fast ice. In the southwestern part of the sea, such ice occupies 55% of the shore fast ice area, and in the northeast, it captures 74% of shore fast ice one (Gabdullin, 2014). For estimation of morphometric characteristics of ice hummocks and level ice 1 time in N years, see Table 7 (Gabdullin, 2014).

Table 7– Morphometric hummock ridge parameter estimates (for whole Kara sea region)

Characteristic	Max	Max	Max	1 time	1 time	1 time	1 time	1 time

	2013	2014	2015	in 5 years	in 10 years	in 25 years	in 50 years	in 100 years
Ice hummock length, m	95	130	185	176	208	248	278	308
Max height of ice sheet, m	3,84	4,8	4,47	4,9	5,3	5,8	6,1	6,5
Average height of ice sheet, m	2,22	3,69	2,27	3,2	3,6	4,2	4,6	5,0
Max width of ice sheet, m	35	48	19	48	59	73	84	94
Ice sheet width, m	35	48	19	48	59	73	84	94
Max cross sectional area of ice sheet, m^2	60	98	65	88	100	114	125	136
Average cross-sectional area of ice sheet, m^2	46	70	48	63	70	79	85	92
Ice sheet volume, m^3	4084	7900	8897	9653	11738	14374	16329	18270
Average ice thickness, m	11,13	10,96	10,01	11,3	11,8	12,5	12,9	13,4
Max cross-sectional area of ice hummock, m^2	500	763	595	732	824	940	1027	1112
Average cross-sectional area of ice hummock, m^2	461	607	457	557	600	655	695	736
Ice hummock volume, m^3	35575	76234	84477	93362	114919	142157	162364	182421
Distance between the points of max ice sheet and max keel, m	54	25	77	77	97	122	141	159
Distance between max section of ice sheet and max section of keel, m	77	68	73	77	80	85	88	92
The ratio of the max keel offset to the length of the ice hummock, unit fraction	0,8	0,6	0,5	0,7	0,8	0,9	1,0	1,1
The ratio of the max section keel offset to the ice hummock width, unit fraction	1,4	1,8	1,6	1,8	1,9	2,1	2,3	2,4
The ratio of the max section keel offset to the ice hummock length, unit fraction	0,9	0,5	0,5	0,8	0,9	1,0	1,0	1,0
Consolidated layer thickness, averaged over sections, m	2,64	1,96	2,06	2,5	2,7	2,9	3,1	3,3
Consolidated layer thickness in max hummock section, m	3,10	2,11	2,16	2,8	3,1	3,4	3,7	4,0
Maximum average consolidated layer thickness over cross sections, m	3,21	2,11	2,19	2,9	3,2	3,6	3,9	4,2
The ratio of consolidated layer to hummock thickness, unit fraction	0,63	0,55	0,40	0,65	0,74	0,86	0,94	1,00

Porosity of nonconsolidated hummock, unit fraction	0,30	0,39	0,44	0,45	0,51	0,58	0,63	0,68
The ratio of the max keel offset to the length of the ice hummock, unit fraction	0,8	0,6	0,5	0,7	0,8	0,9	1,0	1,1
The ratio of the max section keel offset to the ice hummock width, unit fraction	1,4	1,8	1,6	1,8	1,9	2,1	2,3	2,4
The ratio of the max section keel offset to the ice hummock length, unit fraction	0,9	0,5	0,5	0,8	0,9	1,0	1,0	1,0
Consolidated layer thickness, averaged over sections, m	2,64	1,96	2,06	2,5	2,7	2,9	3,1	3,3
Maximum average consolidated layer thickness over cross sections, m	3,21	2,11	2,19	2,9	3,2	3,6	3,9	4,2
The ratio of consolidated layer to hummock thickness, unit fraction	0,63	0,55	0,40	0,65	0,74	0,86	0,94	1,00

Stamukhas

In the Kara Sea, the formation of stamukhas is largely related to the bottom relief. Many stamukhas are formed in the Ob-Yenisei district, the Baydaratskaya Bay, Ob Bay and Tazovskaya Bay, in the Yenisei Bay and Gyda Bay they are formed less often; on the eastern shores of Novaya Zemlya islands, they appear extremely rare. In the coastal zone near the Yamal Peninsula in the shore fast ice, several powerful barriers of ice hummocks and stamukhas are often observed parallel to the coast. In Kara sea stamukhas form mainly from local origin ice, but it was recorded their formation from annual and biennial ice brought from the northeastern part of the sea (AARI, 2017). After breaking of shore fast ice and cleansing the sea from the ice, normally, stamukhas disappear. However, there are cases where stamukhas persisted near Sverdrup Islands until the next winter. In the area of Pobeda field, stamukhas are not observed.

In the Kara Sea, the predominant draft of the stamukhas is 8–12 m; the prevailing height of the ice sheet is 5–10 m. The maximum-recorded stamukha in the Kara Sea was 19x32 km in size; it was located in an area with a sea depth of about 5.5 m and existed for about 5 years.

Figure 5 shows the zones of possible formation of stamukhas.
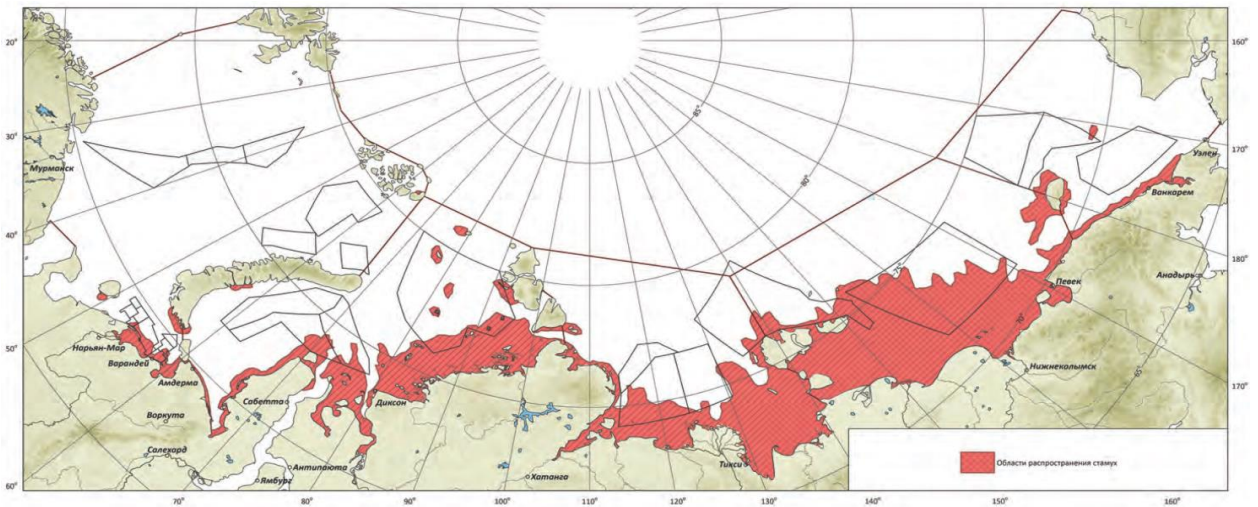
Figure 5 –The zones of possible stamukha formation (Gabdullin, 2014)

Icebergs

In the Kara Sea, icebergs are located adjacent to groups of islands such as Franz Josef Land, Novaya Zemlya, Severnaya Zemlya, Ushakov Island. 83% of all icebergs recorded in the sea are debris and pieces, 10% of them are column-shaped icebergs, 5% of them are collapsing ones, Figure 8. In the Kara Sea, the average size of icebergs comprises the following features: length is 63m, height is about 9m. The maximum length may exceed 150m; the height might reach 30m. From February to May, icebergs are located mainly in the northern part of the sea, Figure 6, near the places of their formation. The maximum number of icebergs in the central part of the sea is observed from July to September.
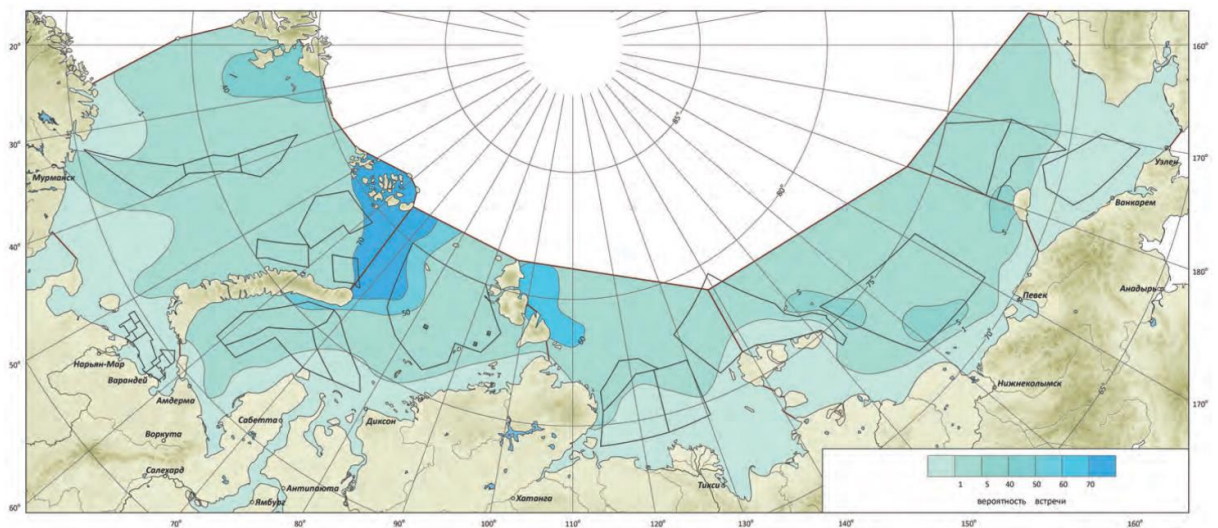
Figure 6 - The iceberg distribution (Gabdullin, 2014)

The spreading of icebergs is chaotic; consequently it can lead to the different trajectories of icebergs. Figure 7 represents possible iceberg trajectories in 2000 and 2003, respectively. It could be noted that the iceberg drift towards the south in year 2003 was exceptional due to strong

winds in southern direction.
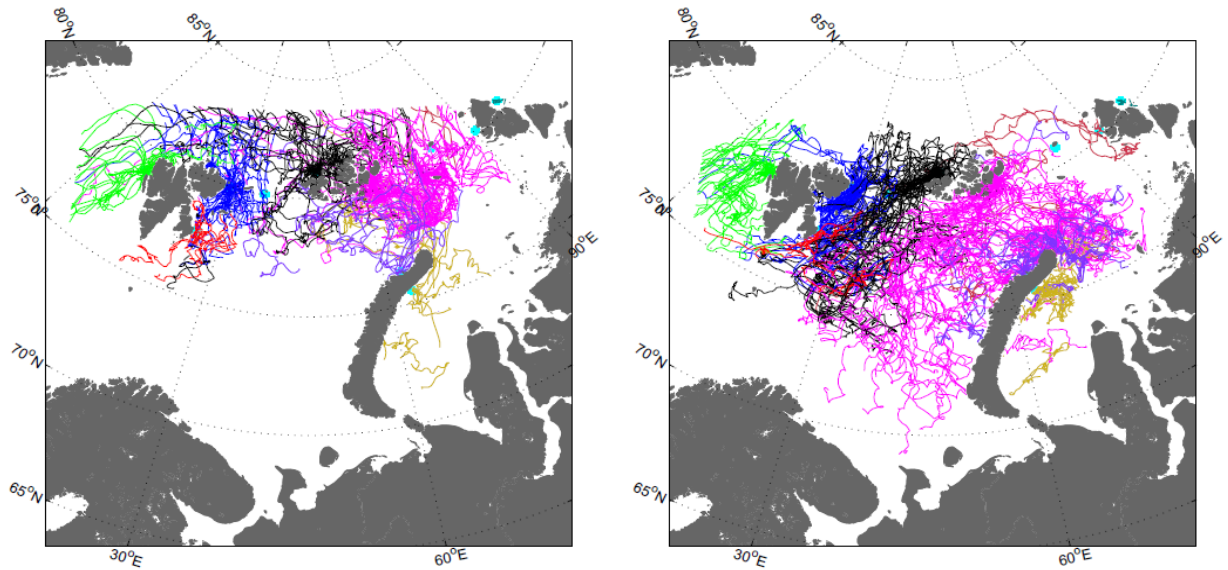
Figure 7 - Iceberg trajectories from the year 2000 and the year 2003 (Keghouche, 2010)

The observations of iceberg drift in the Kara Sea showed that towards northeast is the dominant direction of their movement in the spring and summer. The maximum length of the path traveled by an iceberg per 1 day, 3 days and 7 days was 39.5 km, 98.9 km and 195.2 km, respectively. The average speed of movement was 11 cm/s by maximum 44 cm/s per day, i.e. an iceberg moving can reach 40 km per day (Gabdullin, 2014).

The maximum-recorded drift rate of icebergs at the Pobeda area was 82.2 cm/s in the direction of 156 º, the average speed was 15.6 cm/s. The northeast prevails in the direction of the drift.
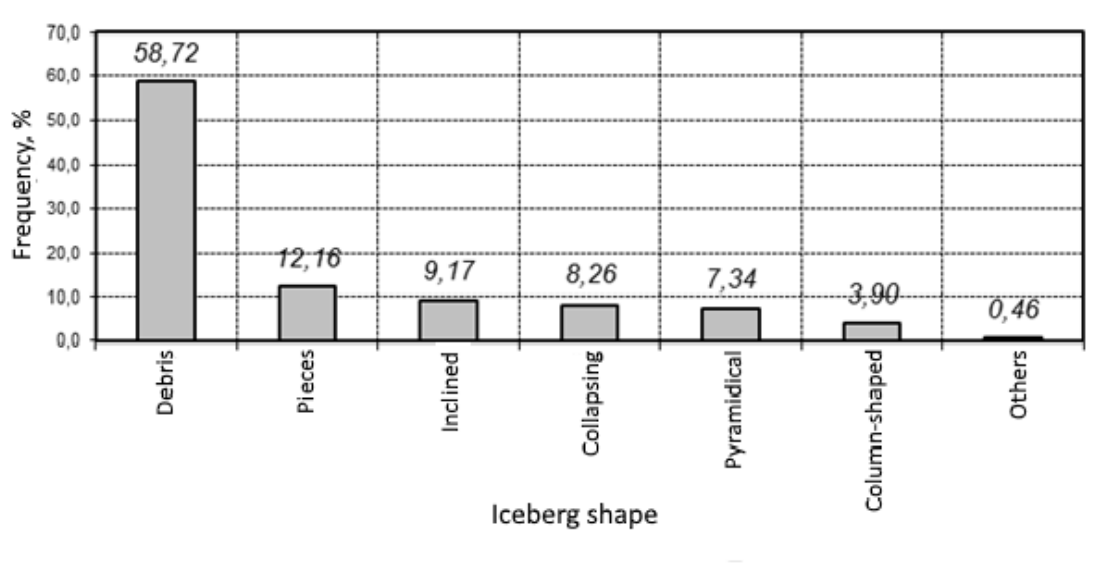
Figure 8 – The iceberg form occurrence frequency distribution in the southwestern part of the Kara Sea (Gabdullin, 2014)

Thus, most often, the southwestern part of the Kara Sea is iceberg-free, but sometimes

there are the fragments of icebergs.

The average expected size of icebergs in the southwestern part of the Kara Sea is 52x31 m, the height is 10 m. Assuming that the underwater part of icebergs is described by a rectangular prism, that is typical for column-shaped icebergs according to observations in the Barents Sea, the average iceberg draft is about 35 m, the maximum one is 77 m. In the area of the Pobeda field, icebergs should be expected with a draft of up to 22 m. According to the definitions, the draft of debris and pieces of icebergs under the assumption that a segment of an ellipsoid describes underwater part, debris' draft does not exceed 20 m (AARI, 2017).

For pipeline design purposes the maximum expected draft has to be taken into account. This means that we either have to route the pipeline into deeper waters (westwards) or to trench the pipeline to a depth where the pipeline will not be overstressed if a deep iceberg occurs at the site. In case of soft bottom conditions, the required trenching depth will be very large (in the order of 5 to 10m). Trench stability will in such cases be an issue.

Grounded icebergs

Mostly, grounded icebergs are placed on shallow waters near Franz Joseph Islands and the north tip of Novaya Zemlya, Figure 9. However, some small portions of grounded icebergs are located at East-Prinovozemelsky site. It is crucial to take into account this issue for safe pipeline route.
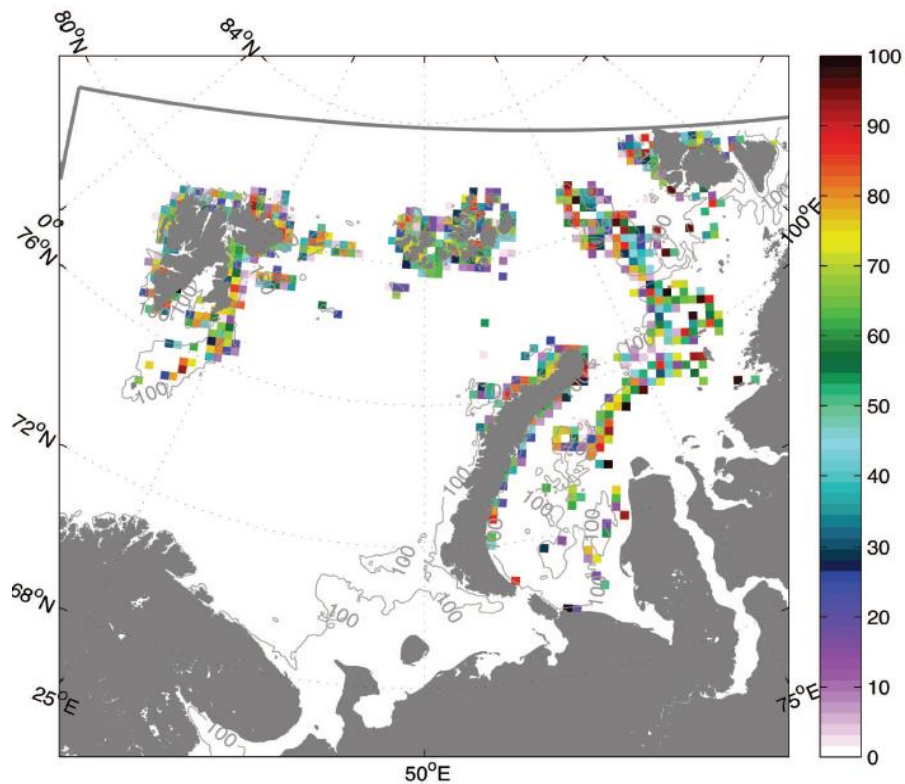
Figure 9 - Probability of a grounded iceberg within a 25 km×25 km (Keghouche, 2010)

Eventually, ice conditions are the most crucial and hazardous compared to other

conditions like wind, waves and etc. The ice environment causes us to design development assets in safe and robust manner taking all aspects of ice and icebergs into account.

In the conditions of the Kara Sea, it is necessary to have reliable ice-resistant bases capable of resisting the loads of moving ice, hummocks and possibly icebergs in harsh arctic conditions. Taking into account the climatic features of the Pobeda field a matrix of applicability of various types of offshore constructions in the Kara Sea was composed, Table 8.

Table 8 – The matrix of applicability of offshore constructions

| Parameters | Artificial island | Piers | | Offshore ice-resistant fixed platforms | | | SPS |
| | | Massive piers | Jacket piers | Jacket platform | Gravity based structures | | Subsea production system |
					Monopod	Multi-legs	
Hydrometeorological conditions:							
Water depth up to 50 m	🔴	🟡	🟡	🟢	🟢	🟢	🟡
Water depth up to 120 m	🔴	🟡	🟡	🟡	🟢	🟢	🟢
Air temperature: 22 - -45°C	🟢	🟢	🟢	🟢	🟢	🟢	🟢
Water temperature: – 1,8-5,0 $^{\circ}$C	🟢	🟢	🟢	🟢	🟢	🟢	🟢
Currents: 5-15 м/с	🟢	🟢	🟢	🟢	🟢	🟢	🟢
Max wave height: 8 m	🟢	🟢	🟢	🟢	🟢	🟢	🟢
Max wind speed: 40m/s	🟢	🟢	🟢	🟢	🟢	🟢	🟢
Farness of onshore infrastructure							
Distance to onshore assets: 400 km	🔴	🟡	🟡	🟢	🟢	🟢	🔴
Ice conditions							
Ice period: 240 days	🟢	🟢	🟢	🟢	🟢	🟢	🟢
Ice thickness: 120-160 cm	🟢	🟡	🟡	🟡	🟢	🟢	🟢
Icebergs	🔴	🔴	🔴	🔴	🟡	🟡	🟡
Max ice hummock width: 25 m	🟡	🔴	🔴	🔴	🟢	🟢	🟡
Platform topside							
One derrick	🟢	🟢	🟢	🟢	🟢	🟢	-
Two derricks	🟢	🟢	🟢	🟢	🔴	🟢	-
Oil process facility	🟢	🟢	🟢	🟢	🟢	🟢	-
Oil storage	🟢	🔴	🔴	🔴	🟢	🟢	-
Offloading to tankers	🔴	🔴	🔴	🔴	🟢	🟢	-
Gas process facility	🟢	🟢	🟢	🟢	🟢	🟢	-
Gas shipping to the onshore by pipeline	🟢	🟢	🟢	🟢	🟢	🟢	-

🔴 not admissible; 🟡 admissible under defined circumstances; 🟢 admissible

Chapter 2. The choice of offshore structure

In accordance with given natural conditions, types of oil platforms applied to mild conditions in temperate zones and seas not covered by ice are not taken into consideration. In this work, severe conditions of the Arctic region in Kara Sea where the Pobeda field is situated are essential. Next step is to review the types of petroleum platforms and their assemblies intended for utilization in the Arctic seas, namely offshore ice-resistant fixed platform. This type of offshore constructions should overcome harsh climatic conditions in Arctic region. Thus, this platform must have a certain stock of resources, energy, durability, comfortable and safe working conditions for its staff and workers involved in oil and gas extraction because the costal infrastructure in the areas of running of these faculties is poorly developed or not developed at all. In that regard the reliability of the faculties, their safety and the ability to withstand the harsh climatic conditions of the Arctic seas are indispensable requirements for this platform types.

In accordance with (Borodavkin, 2006), the following characteristics of the environment affecting the platform choice for oil and gas extraction are highlighted:

- State of the surface of the marine environment. Here it is reviewed the possible state of water near the sea surface in different periods of the year: the sea may be non-freezing (the sea surface does not freeze) or freezing (the sea surface is covered by ice). In our case, we are dealing with frozen seas. In that regard, we should pay attention to the possible ice pressures that the oil platform will have to obtain.

- Sea depth. The depth of the sea will influence the choice of the platform structure at its location. It is customary to divide the depths into large, medium and small. According to the hydrological interpretation, marine areas can be divided into deep-sea, shallow-water and coastal areas, depending on wave's changes as the water depth changes.

- Geological structure of the seabed. The method of fixing the oil platform will depend on the bearing strength of the soil in the place of the platform installation (compliant tower platform, gravity-based platform and etc.).

- Hydrodynamic characteristics of the sea. It should include concepts such as fluctuations in the level of the sea surface (daily, seasonal, annual, etc.), constant currents and currents typical for different periods of the year, cyclic and random variations of the sets of the currents. In addition, waves and their shape, periodicity, height and length have the particular importance for determining the parameters of the constructions.

- Wind characteristics in the area of construction of the platform. Wind forcing is manifested in two main pillars. The first one is the direct force action on the open parts of the oil platforms; the second is the disturbance of the surface of the sea and the

emergence of wind waves and temporary current. It in turn directly affects the construction located in water.

- Seismic attributes in the area of the location of offshore constructions. Seismic load is a very significant factor affecting the facility as a whole. Seismic loads are characterized with intensity and repetition frequency for a period not less than 100 years.

- Thermal behavior of the environment. Thermal behavior is the regularity of possible temperature fluctuations of the environment by seasons. The maximum and minimum temperatures are set. The awareness of the thermal behavior of the environment allows to avoid process disturbances as a result of freezing of water or hydraulic fluid, allows to insulate premises where people should work and also, allows to provide people with the necessary working clothes suitable for a particular temperature and climatic period.

In addition, the possible icing-up of the parts of the offshore construction can affect significantly at temperatures below or close to zero. In turn, it can weigh the construction and even lead to the shift of estimated centers of gravity, which can lead to a decrease of structure stability.

Ice condition at the installation area or in the vicinity of field is the main factor which influences the design, fabrication, transportation and exploitation of ice-resistant offshore platforms for Arctic seas.

Due to the remoteness of the field from the coastal infrastructure and the harsh conditions of the Arctic region, the required offshore construction should have a number of properties and perform a full range of functions which are necessary for the full and effective field development. The offshore structure should ensure the implementation of processes related to production, storage and treatment of oil and gas, comfortable and safe living and work conditions for the staff. The construction should have the necessary equipment for drilling both wildcats and production well and an equipment for the vessel mooring.

In addition, in this case it is more expedient to use offshore constructions fixed on the seabed by means of supportive blocks of a particular configuration. Such constructions can transfer loads from the weight of the structure and its equipment to the soil, transfer impacts from environmental factors: wind, waves, currents and ice pressure (Huaiyin et al., 2015).

Regarding the appropriateness of bottom supported facilities, several versions of platforms will be reviewed (Eie et al., 2014), namely: point-supported or mono-supported structures (a structure supported on the bottom of the sea or is fixed to the bottom at one point), multi-legged structures (structures supported on the bottom of the sea with several support structures), in the form of a caisson (structures in the form of a huge block of concrete, metal, stone or soil).

Subsea production systems are not taken into consideration as a separate group of possible offshore facilities because of their inability to provide a full cycle of work on the field but SPS can only be used jointly with platforms as a part of the system of facilities for oil and gas production. In addition, these faculties bring a huge danger of the pollution of the marine areas in case of an accident that is very dangerous for the ecosystem of the Arctic seas.

The platform topside is also very important under construction of the ice-resistant platform. The topside of the platform houses the technological equipment, power plants, household premises (aimed of 200-300 people), warehouses located in block-modules installed in several floors. There are also drilling and flare stacks, cranes and helideck on the topside of the platform.

The following table (Table 9) is a comparative analysis of the Kara Sea conditions and the Pobeda field with the analogues of offshore ice-resistant fixed platform exploited in other seas.

Table 9 – Comparative analysis of existing projects

Item #	Kara Sea and "Pobeda" field parameters	Kara Sea and "Pobeda" field parameters — Parameter value	Orlan (Okhotsk Sea)	Berkut (Okhotsk Sea)	Piltun-Astokhskaya - A» (Molikpak) (Okhotsk Sea)	Piltun-Astokhskaya-B» (PA-B) (Okhotsk Sea)	Lunsakay - A (LUN-A) (Okhotsk Sea)	Prirazlomnaya (Barents Sea)	Troll - A (North Sea)	GULLFAKS (North Sea)	DRAUGEN (North Sea)	Statfjord-B (North Sea)	Ice resistant fixed platform (LSP-1 & LSP-2) (Kaspian Sea)	Hibernia (Atlantic Ocean)	Hebron (Atlantic Ocean)	Ice resistant fixed platform D-6 (Baltic Sea)
													Parameter value on analogue platforms / Types of platform design / Sea			
1	The sea depth at the drilling / installation, m	**50**	15	35	30	32	48	20	350	217	250	145	11-13	80	92	25-38
2	Ice:															
3	Duration of ice cover, mon.	**8 -9**	8	8	8	8	8	9	-	-	-	-	5	7-8	7-8	3-4
4	Thickness of the ice cover, m:															
5	Multi-year	**2**	2,2	2,2	2,2	2,2	2,2	Up to 3	-	-	-	-	-	-	-	-
6	First-year	**1,6**	0,9-1,3	0,9-1,3	0,9-1,3	0,9-1,3	0,9-1,3	Up to 1,5	-	-	-	-	0,8	0,6 - 0,8	0,6 - 0,8	0,5 - 0,8
7	The presence of icebergs	**Yes**	No	No	No	No	No	No	No	No	No	No	No	Yes	Yes	No
8	The presence of other ice bodies (hummocks, layered ice, etc)	**yes**	yes	Yes	Yes	yes	Yes	yes	No	No	No	no	Yes	yes	Yes	Yes
9	Average annual air temperature, deg, C:															
10	Maximum	**8 - 31**	28-32	28-32	28-32	28-32	28-32	8,8	23-25	23-25	23-25	23-25	37	10-17	10-17	23-24
11	Minimum	**-44 – (-48)**	-36 – (-45)	-36 – (-45)	-36 – (-45)	-36 – (-45)	-36 – (-45)	-19,0	3 - 4	3 - 4	3 - 4	3 - 4	-22	- 3 – (-17)	- 3 – (-17)	-18 – (-25)
12	Significant height of waves, m	**4,7-8,2**	9,0-11,2	9,0-11,2	9,0-11,2	9,0-11,2	9,0-11,2	2,5	2-7	2-7	2-7	2-7	1,3	3-7,5	3-7,5	5
14	Volume of mineral reserves:															
14	Oil	**130 mln.t.**	31,938 mln.t.		125,2 mln.t.	125,2 mln.t.	124,465 mln.t.	46,4 mln.t.	from 250 to 750 mln.t.	200 mln.t.		500 mln.t.	28,8 mln.t.	420 mln.t.	98 mln.t.	9,1 mln.t.
15	Gas	**499,2 bcm**	9,9 bcm		102,8 bcm	102,8 bcm	526,7 bcm		1,3 tcm	200 bcm		200 bcm	63,3 bcm	-	-	-
16	Distance from the shore or transport systems	**250 km**	12 km	About 25 km	16 km from	About 12 km from	15 km	60 km from the coast	100 km Northwest of Bergen	160 km from the Sognefjord		200 km West of Bergen	180 km from Astrakhan	315 km	350 km from St-John's	22,5 km from the cost

According to the analysis presented in Table 9, it can be concluded that for the development of the Pobeda field (by natural and logistic characteristics), the utilization of existing analogues can be ranked as follows:

Hibernia and the Hebron project are suitable for many basic natural conditions present at the Pobeda field in the Kara Sea such as the depth of the sea at the installation point, the duration of the ice cover, the ice thickness, the presence of icebergs and other ice bodies, the wave height, the volume of reserves, and the distance from the shore and transport systems.

The following group includes Sakhalin projects located in the Okhotsk sea in the form of platforms Orlan, Berkut, Piltun-Astokhskaya-A (Molikpak), Piltun-Astokhskaya-B (PA-B), Lunskaya-A (LUN-A). They are also suitable for many basic natural conditions at the Pobeda field in the Kara Sea, namely: the duration of the ice cover, the ice field thickness, the presence of different ice forms, the volume of mineral reserves, and the average annual negative air temperature.

The offshore ice-resistant fixed platform Prirazlomnaya in the Barents Sea is suitable for the following factors: the duration of ice cover, the ice field thickness, the presence of ice forms.

The offshore ice-resistant fixed platforms in Caspian and Baltic Sea, Troll-A, GULLFAKS, DRAUGEN, Statfjord-B, located in the North Sea are not suitable for the Kara Sea conditions.

Eventually, next analogues for the possible development of the Pobeda field will be discussed (Figure 10):

Figure 10 – Possible analogues for Pobeda field development

For the Pobeda field in the Kara Sea the architectural and layout schemes of platforms in concrete and steel execution are proposed. The support block provides the possibility of arrangement of oil storage capacity of up to 150000 m^3. Massive supporting constructions in the form of a monopod, slope structure or multi-legged structures are suitable for given oil/gas filed.

Under the conditions of the Pobeda field, the major disadvantage of monopod and slope structure (Figure 11) is the inability to locate two derricks for drilling a large number of wells from the platform (Gabdullin, 2014). Thus, the analogue of Prirazlomnaya platform is not taken
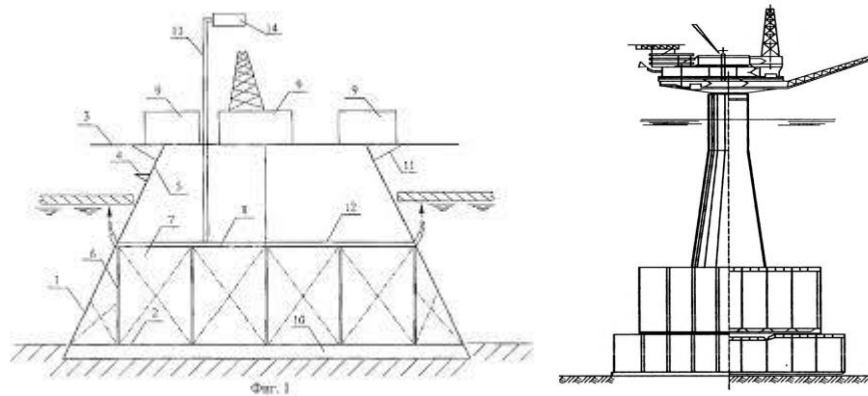
into account.

Figure 11 – The scheme of slope structure and monopod structure (All patents, 2015)

As an alternative, the gravitational based structure of the multi-leg type (4 columns) is proposed (Figure 12).
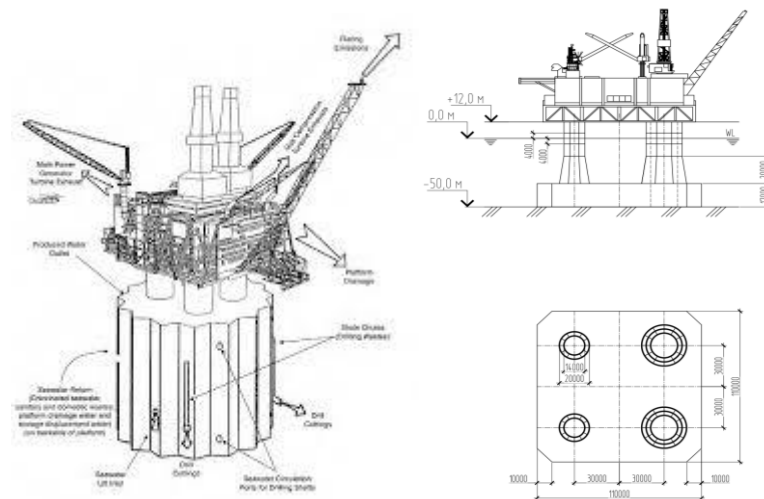

Figure 12 – Multi-leg gravity fixed structure for Pobeda field (Stantec, 2013)

The support ice-resistant block of gravity type shall be made of reinforced concrete. Reinforced concrete blocks of gravitational type are usually constructed in drydock. After manufacturing of foundation (caisson) with oil storage unit, it has been brought to the deep waters and continues the construction of the vertical columns (shaft) afloat. There is also a possibility of the towing and installation of a complete platform in the field. The supporting caisson has the form of a rectangle or 16-pointed star. It is divided by waterproof partitions into compartments, which provide buoyancy during sea operations and installation of the offshore ice-resistant fixed platform on the field.

In the caisson of Gravity Based Structure (GBS), there are also located concrete tanks for oil storage, diesel fuel, fresh water, etc. In the lower part of the supporting caisson there is a system of crisscrossing steel skirts embedded in the base plate and buried in the ground under the own weight of the platform.

The four supporting columns of the GBS are subdivided into:

- 2 columns in which guide conductors for oil and gas wells are placed;
- 1 column, where riser pipes, gaslift pipelines, flexible drill strings are stored;
- 1 column, in which there are pipelines for seawater collection for technological needs and for fire extinguishing system of the platform, pipelines for the disposal of treated wastewater and disposal of neutralized household waste, etc.

The support block with topside is planned to install on the seabed by ballasting the support base with seawater. After installation on the perimeter of the base, the multilayer protection (stone berm) is arranged to prevent erosion of the seabed under the caisson. The topside is structured for the allocation of the complexes of the technological and power equipment, accommodation block and other systems. Each technological complex of the platform includes a number of systems. The main complexes on the Pobeda offshore ice-resistant fixed platform:

1. Drilling complex. There are two drilling complexes for the drilling of wells of oil and gas deposits:

2. Complex providing the multi-stage hydraulic fracturing;

3. Technological complex;

4. Energy complex;

5. Complex of control systems;

6. Life support and accessory systems complex.

The calculation of ice load

Next stage will be calculation of ice cover load to GBS. The ice-structure interaction nature complexities, as well as the features of the physicomechanical ice properties, are the main reason for the lack of rigorous theoretical solutions, which make it possible to accurately determine the ice loads for almost all cases. Now there are a large number of regulatory documents and recommendations, where the estimated value of ice load is utilized with various assumptions. In this master thesis there are applied two standards for the ice load calculation:

- (SP, 2012);
- (ISO, 2010).

Firstly, calculation will be performed for multi-legged structure Lunskaya platform type, namely the ice cover interacts with columns.

For this thesis, it is assumed that there is no snow on the ice surface. Air temperature (T_{air}) is -24°C. Salinity ($s_{w,t}$) of ice is 6‰. Use formula for the calculation of ice load impact:

$$F_{b,h} = m * k_b * k_v * R_c * b * h_d$$

R_c – ice compression strength;

m – The coefficient of the form of platform support (taken from table);

k_b – crumpling coefficient (taken from table);

k_v – ice deformation rate coefficient (taken from table);

b – The leg width (according to Lunskaya platform -22m)

h_d – ice field thickness (from the first chapter it is 1,6m).

Firstly, it is necessary to define ice compression strength using formula:

$$R_c = \sqrt{\frac{1}{N} \sum_{i=1}^{N} (C_i \pm \Delta_i)^2}$$

Where N is a number of layers with the same thickness (take N=4);

C_i – the value of ice strength in i-th layer by i-th temperature;

Δ_i – the confidence limit of error.

Ice cover is separated for four equal parts. Each part is 0,4m. As there is no snow on the ice field surface, it is assumed that the temperature of top ice-edge is equal to air temperature (T_{air} = -24°C). The temperature of low ice-edge is -1,8°C. The ice temperature through thickness alters linearly, thus there is next temperature distribution:

- The first layer: T_1= -21,6°C;
- The second layer: T_2= -15,8°C;
- The third layer: T_3= -10°C;
- The fourth layer: T_4= -4,2°C.

Then we should determine the amount of liquid phase in the i-th layer of the ice field.

$$\xi_i = -\frac{s_{w,t}(1-0,018t_i)}{0,018t_i}, \quad 0\,°C < t_i < -7,3\,°C;$$

$$\xi_i = -s_{w,t}\frac{1,06-0,005t_i}{0,03-0,014t_i}, \quad -7,3\,°C < t_i < -22,4\,°C;$$

$$\xi_i = -s_{w,t}\frac{1,17-0,005t_i}{2,0-0,106t_i}, \quad -22,4\,°C < t_i < -30,0\,°C,$$

Figure 13 – The formulas for liquid phase amount definition (SP, 2012)

where $s_{w,t}$ is ice salinity; t_i is the temperature of i-th layer.

$$\xi_1 = -6 * \frac{1,06 - 0,005 * (-21,6)}{0,03 - 0,014 * (-21,6)} = 21,1$$

$$\xi_2 = -6 * \frac{1,06 - 0,005 * (-15,8)}{0,03 - 0,014 * (-15,8)} = 27,2$$

$$\xi_3 = -6 * \frac{1,06 - 0,005 * (-10)}{0,03 - 0,014 * (-10)} = 39,1$$

$$\xi_4 = -6 * \frac{1 - 0,018 * (-4,2)}{0,018 * (-4,2)} = 85,4$$

Using tables in (SP, 2012) we get the values for $C_i \mp \Delta_i$:

$$C_1 \mp \Delta_1 = 4,1 \pm 0,6$$
$$C_2 \mp \Delta_2 = 1,8 \pm 0,3$$
$$C_3 \mp \Delta_3 = 1,2 \pm 0,1$$
$$C_4 \mp \Delta_4 = 0,5 \pm 0,1$$

$$R_c = \sqrt{\frac{1}{N} \sum_{i=1}^{N} (C_i \pm \Delta_i)^2} = \sqrt{\frac{1}{4} * (4,7^2 + 2,1^2 + 1,3^2 + 0,6^2)} = \sqrt{7,1} = 2,67 MPa$$

$m = 0,83$ (semi − circular outline); $k_b = 1,2$; $k_v = 1$ thus

$$F_{b,h} = m * k_b * k_v * R_c * b * h_d = 0,83 * 1,2 * 1 * 2,67 * 22 * 1,6 = 93,6 \, MN$$

For four supports with span 36m between each other, ice load is calculated by formula:

$$F_p = n_t K_1 K_2 F_{b,h}$$

Where n_t is a number of columns,

K_1 – peak load value coefficient (taken from table);

K_2 – the coefficient of mutual influence between supports (taken from table).

$$K_1 = 0,83 + 0,17 * n_t^{-0,5} = 0,83 + 0,17 * 4^{-0,5} = 0,915;$$

$$K_2 = 0,55 + 0,45 * \frac{k_n}{k} = 0,55 + 0,45 * \frac{0,4}{0,575} = 0,86.$$

$$F_p = 4 * 0,915 * 0,86 * 93,6 = 294,6 MN$$

For compartment, it is possible to use (ISO, 2010). In accordance with this document, there is a formula:

$$F_g = p_g * b * h$$

- The first variable is an average value of the ice scale pressure (MPa);
- The second variable is the design width of offshore structure (m);
- The third variable is ice cover thickness (m).

Firstly, it is necessary to find the value of ice scale pressure:

$$p_G = \left\{ C_R * \left(\frac{h}{a}\right)^n * \left(\frac{b}{h}\right)^m \right\} = 2,8 * \left(\frac{1,6}{1}\right)^{-0,16} * \left(\frac{22}{1,6}\right)^{-0,30} = 1,18 \, MPa$$

Where "a" is the reference value of ice thickness equals 1m;

"C_R "is the ice strength coefficient (MPa). For arctic areas it is 2,8;

"n" is the empirical coefficient. It is -0,16;

"m" is the empirical coefficient. It is -0,30 for h>1m.

Calculate ice field load for one vertical platform column

$$F_g = p_G * b * h = 2,8 * \left(\frac{1,6}{1}\right)^{-0,16} * \left(\frac{22}{1,6}\right)^{-0,30} * 22 * 1,6 = 41,6 \ MN$$

For four supports with span 36m between each other ice load is calculated by formula from (ISO, 2010):

$$F_s = k_s k_n k_j F_g$$

Where k_s – the coefficient of interference and sheltering effects (taken 3,25);

k_n – the coefficient of the effect of non-simultaneous failure (taken 0,9);

k_j – the coefficient of the ice jamming (taken 1).

$$F_s = 3,25 * 0,9 * 1 * 41,6 = 121,8 MN$$

Secondly, calculations will be performed for Hibernia platform type. This platform has 16-point star caisson with diameter 108m (Matskevitch, 2005). For the simplicity of calculation assumptions are introduced, namely ice cover interacts only with 1-point section of caisson and sharp tip of star caisson is changed by inscribed circle with appropriated radius 18,8m (Figure 14). Orange curve is imaginary circle, restricted by two ribs of triangle.
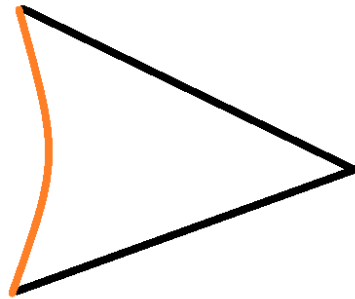

Figure 14 – Change triangle tip by circular shape

In accordance with previous step of ice cover load calculation by (SP, 2012), there is next value:

$$F_{b,h} = m * k_b * k_v * R_c * b * h_d = 0,83 * 1,2 * 1 * 2,67 * 18,8 * 1,6 = 80 \ MN$$

In accordance with previous step of ice cover load calculation by ISO 19906, there is next value:

$$p_G = \left\{ C_R * \left(\frac{h}{a}\right)^n * \left(\frac{b}{h}\right)^m \right\} = 2,8 * \left(\frac{1,6}{1}\right)^{-0,16} * \left(\frac{18,8}{1,6}\right)^{-0,30} = 1,24 \ MPa$$

$$F_g = p_G * b * h = 2,8 * \left(\frac{1,6}{1}\right)^{-0,16} * \left(\frac{18,8}{1,6}\right)^{-0,30} * 18,8 * 1,6 = 37,3 \, MN$$

Table 10 – The comparison of ice load values depending on structure under different standards

Platform support//Standard	Four-leg support	Massive caisson
SP 38.13330.2012	294,6 MN	80 MN
ISO 19906	121,8 MN	37,3 MN

The Russian and foreign norms for ice load calculation on the ice-resistant fixed platform are based on various approaches to assess their reliability. As a result of the comparison, it is impossible to make a conclusion about the fundamental superiority of one of the methods over the others.

To understand which result is closer to the truth, it is necessary to take into consideration experimental results made by T.D. Sanderson (Figure 15).
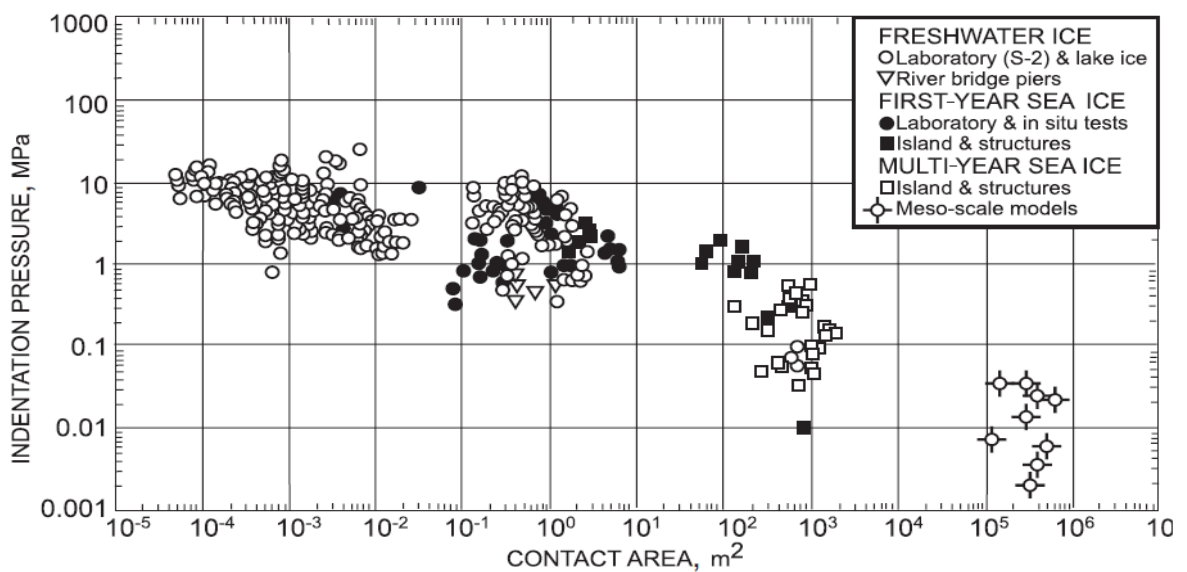

Figure 15 – Sanderson's chart (Løset et al., 2006)

According to Sanderson's graph, when the area of ice exposure as more than 10^2 m^2 the value of ice scale pressure rarely exceeds 2 MPa. Using formula from (SP, 2012), it revealed an ice load which is equal 294 MN and 80 MN by an average ice pressure of 2,67 MPa. The calculations are clearly overestimated due to the revaluation of the average ice pressure. In order to reduce the calculated ice pressure, it is necessary to clarify: the temperature profile of ice (to take into account the layer of snow), the structure of ice, the salinity profile of ice through-thickness.

For modelling of ice load, the ice load values calculated in accordance with ISO 19906 are taken as more realistic values. Figure 16 gives modelling for two types of platforms.
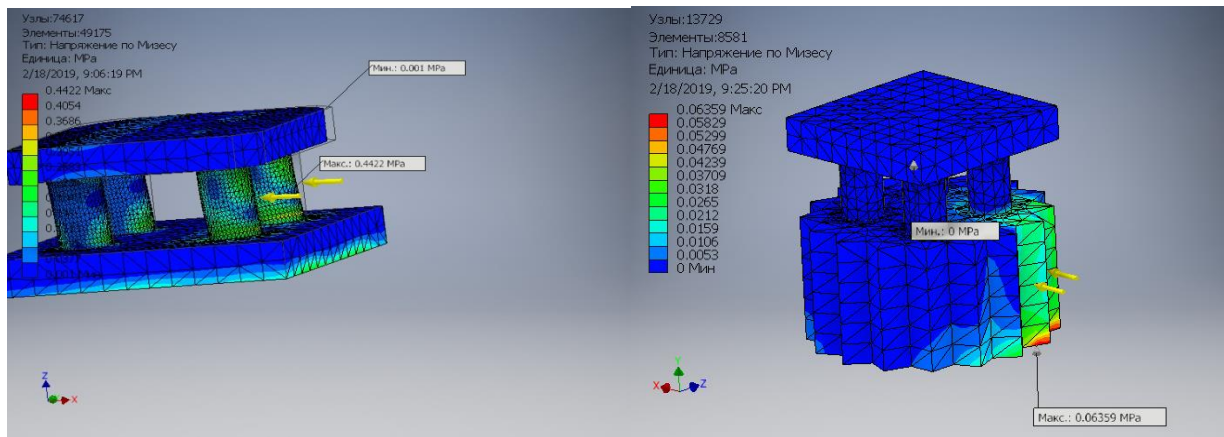
Figure 16 – Stress modelling of support blocks with topside

Four-legged structure can withstand ice cover load and maximum stress equals 0,44 MPa, whereas the structure with massive caisson gets maximum stress which equals 0,06 MPa. The stress in the second case is lower due to 16-point star shape which crashes ice and distributes load from ice cover. Moreover, massive caisson can withstand iceberg impact load is 500 MN for the 500-year event (no damage) and 1300 MN for the 10000-year event (survive with no loss of life or damage for environment) in accordance with (Matskevitch, 2006).

Eventually, a platform type with massive caisson is the most suitable for Pobeda oil/gas field for successful field development in harsh natural conditions. Below (Figure 17) the methodic of the choice of ice-resistant fixed platform support block type is presented.
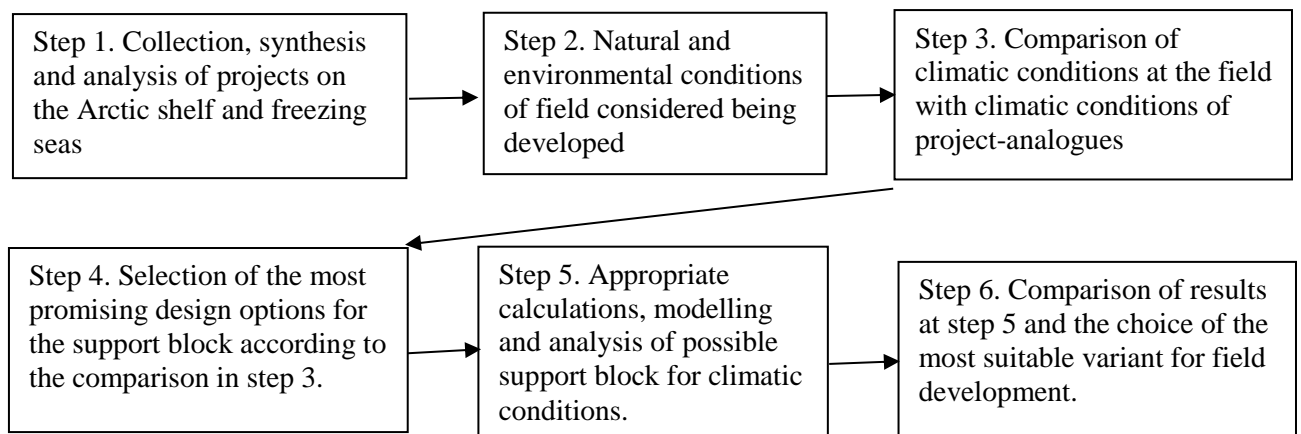
Step 1. Collection, synthesis and analysis of projects on the Arctic shelf and freezing seas → Step 2. Natural and environmental conditions of field considered being developed → Step 3. Comparison of climatic conditions at the field with climatic conditions of project-analogues

Step 4. Selection of the most promising design options for the support block according to the comparison in step 3. → Step 5. Appropriate calculations, modelling and analysis of possible support block for climatic conditions. → Step 6. Comparison of results at step 5 and the choice of the most suitable variant for field development.

Figure 17 – The block-scheme of ice-resistant fixed platform support block choice methodic

Chapter 3. Pipeline hydrocarbon transportation

As it was mentioned in previous chapters, Pobeda field possesses a significant reserve of hydrocarbons. The development of Pobeda field involves transportation systems for oil and gas. It can be implemented by tankers shipping or by subsea pipeline system.

First of all, it is necessary to separate hydrocarbons for the items of produced stuff. Oil is proposed to be delivered by tanker shipping due to low extraction index and the absence of existing infrastructure for oil processing and trading (Gabdullin, 2014).

Gas transportation can be performed the following ways:

- FLNG installation and next offloading to gasholder shipping vessels;
- Gas pipeline construction.

The first way is not suitable due to the absence of technology for ice-resistant FLNG construction. An alternative way is to construct a pipeline from Pobeda field to the onshore facility on Yamal peninsula or Novaya Zemlya Island. However, the pipeline application is associated with various difficulties, such as on-bottom instability, uncontrolled buckling, suitable and cost-effective type of pipeline laying. In order to provide feasible and economically stable development of the Pobeda field pipeline, the following key issues require detailed investigations:

• Seabed survey;

• Pipeline design;

• Pipeline installation method;

• Route selection.

Each section will be described and special attention will be directed to route selection. Pipeline installation may generally comprise curved sections in the horizontal plane, due to natural seabed characteristics. In this part, pipelaying in curve with on-bottom stability consideration using SIMLA software will be presented.

3.1. Seabed survey

In order to choose suitable and appropriate route at the Pobeda field, detail seabed properties and features are of major importance. For pipeline engineering in such area with severe natural conditions, seabed data with high precision and good quality should be obtained as soon as possible in the design process stage.

The sea is located within the continental shelf; therefore about 70% of its area is less than 100 m deep and only 2% is more than 500 m deep. There are two natural troughs: Saint Anna Trough (along the east coast of Franz-Josef Land 600m deep) and Voronin Trough (along the west coast of Severnaya Zemlya 400m deep). The depth contour of the Kara Sea is uneven. In the North-Western part of the site, the average sea depth is 250 m, in the South-West where Pobeda filed is located is up to 100m (AARI, 2017). Figure 18 shows Kara Sea bathymetry.
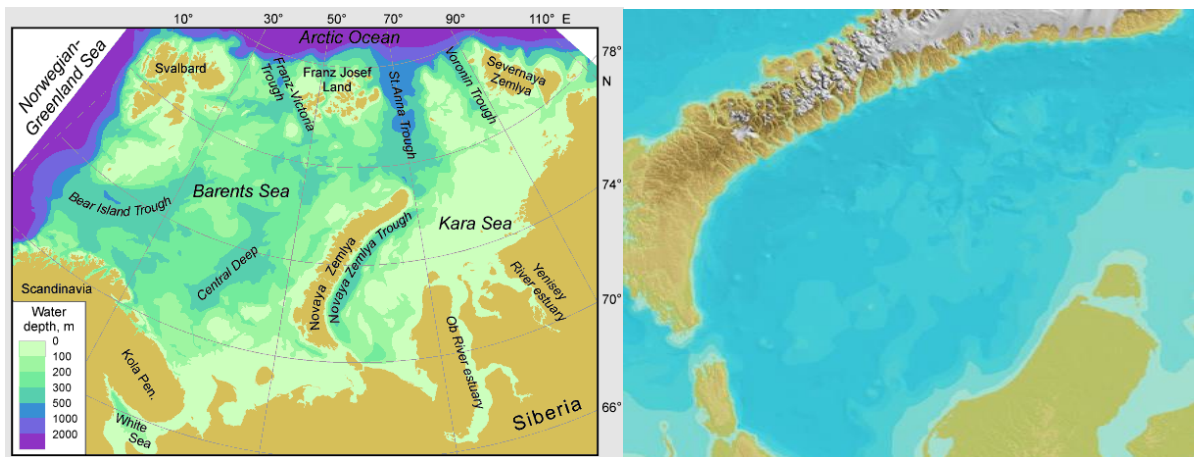

Figure 18 – The bathymetry of Kara Sea (Arctic atlas, 2001)

The seabed is overlain by clayey silts. In the upper part of the section, up to 7-11 m from the bottom, silt clay and loamy, plastic sandy loam and fluidized plastic, belonging to the category of soft soils are laid. A refractory loam has sufficiently high strength characteristics (10 to 15 m from bottom). Semi-solid loam is distinguished by the greatest strength characteristics. It was uncovered at a depth of 15 m and drilled to a depth of 50 m, which is the interbreeding of loams with layers of dusty sand (AARI, 2006).

According to the engineering survey results, there is a number of major uplifts of round shape allocated in the depth contour, with a diameter of 400 m. In accordance with the appearance and size, they resemble the injection swelling bumps (hydro-laccolites, "ping-like structures"). Permafrost ice soils are widespread in shallow areas of the Kara Sea shelf.

Due to the severe ice conditions, there may be a number of negative forms of relief identified– exaration furrows that occur in the shallower part of the landfill. The sizes of furrows vary from 400 meters to 1400 meters in length, from 20 meters to 80 meters in width, depth to 5 meters. The average number of furrows per unit area is 1 piece/km^2 (Gabdullin, 2014).

3.2. Pipeline design

The pipeline should possess necessary technical properties in order to supply gas from oil/gas field to onshore facilities by feasible way. A pipeline material data is necessary for the pipeline design. Due to existing loads acting during operation and installation phases submarine pipelines have to overcome the adverse effect of transported fluids and external environment. Largely this should be provided by the design of the pipeline material. According to (DNV, 2012), materials which are applied in petroleum subsea pipelines are described by the following considerations:

• Mechanical properties;

• Hardness;

• Fracture toughness;

• Fatigue resistance;

• Weldability;

• Corrosion resistance.

The pipeline can get hoop stress, longitudinal stresses, bending and elongating. This behaviour is characterized by hardness which means an ability to consume overstresses with help of deformations. This is one of the major mechanical features of materials, defining the general design (Bai, 2005). The pipeline material should also possess adequate toughness which determines the ability of resistance to immediate impacts (for instance, dropping objects or trawl impact). Fatigue resistance implies the material tolerance to cycling loads which can lead to slow deterioration in the pipeline steel (Karunakaran, 2018). The weldability of a material refers to its ability to be welded with the saving of equal mechanical properties spreading the overall pipeline length. It is important to remember that there is no best steel which is suitable for all requirements. There is always a dependency between properties mentioned above.

The pipeline is proposed to be manufactured from carbon-manganese steel (C-Mn) as the most commonly used competitive material. This steel is suitable for the construction of pipelines (Palmer et al., 2008). It comprises various alloying ingredients, such as carbon (0,10% - 0,15%), manganese (0,80%), silicon, phosphorus, sulphur, nickel and chromium (Karunakaran, 2018). The presence of content of different alloys determines the steel grade and thereafter strength, hardness and other mechanical properties. The major drawback of carbon steel is a poor corrosion resistance (Palmer et al., 2008). It may be improved by adding corrosion resistant materials (martensitic, duplex, austenitic stainless steels) that afford the material to become a CRA (corrosion resistant alloy). Other decision is the usage of external or internal protection, cathodic protection or external coating.

The selection of steel grade is governed in mentioned above properties by the following

factors (Karunakaran, 2018):

- • The price;
- • Weight requirement;
- • Welding Restrictions;
- • Limited Offshore Installation Capabilities.

In accordance with (API, 2000) there are different types of steel up to X80 grade which are presented in table 11.

Table 11 – API material grades (API, 2000)

API grade	SMYS, MPa	SMTS, MPa
X42	289	413
X46	317	434
X52	358	455
X56	386	489
X60	414	517
X65	448	530
X70	482	565
X80	551	620

Steel with high grade offers thinner wall thickness, but manufacturing costs are higher and weldability is decreased. Mostly, high grade steel pipeline is applied for deep-water areas (Bai, 2005).

C-Mn steel pipeline manufacturing is divided into some types of producing processes, affecting the possibility of wall thickness, allowable diameter consideration and cost. There are several types:

- • *Seamless (SMLS)* – manufacturing of seamless pipelines is carried out without welding by a hot forming process. In this case there are no welds, but such pipelines are expensive and have restrictions for diameter (16 inch);
- • *Submerged arc welding – longitudinal seam (SAWL)* – SAWL pipes fabrication is made either by UOE or JCOE processes. These are excellent pipes for big diameter and high-pressure pipelines in terms of good out-of-roundness (+/- 1%) and wall thickness tolerance (Palmer et al., 2008);
- • *Submerged arc welding – helical seam (SAWH)* – SAWH pipelines are applied with a big diameter for oil and gas transportation. Wall thickness tolerance is nearly similar to SAWL pipelines, but ovality is often higher, and long welds are exposed to corrosion, which is aggressive at bottom areas (Palmer et al., 2008);

- *High frequency welded (HFW)* – There is applied high current welding and rolling process. Desirable diameter and wall thickness are achieved by hot stretching and cold expansion. These pipelines are designated for middle diameters (up to 26 inches).

For given conditions at Pobeda field it is proposed C-Mn steel pipeline which has grade steel X60, wall thickness 22mm, outer diameter 1020 mm and is fabricated by UOE SAWL method. Such pipeline characteristics will afford stable and robust natural gas transportation from field to onshore base. Below there will be calculations for checking of stress design. The information about pipeline properties for Pobeda field is given in Table 12.

Table 12 – Pipeline properties

Parameter	Value
Steel grade	X60
Density	7850 kg/m^3
SMYS	414 MPa
SMTS	517 MPa
Elasticity modulus	2,07*10^5 MPa
Poisson ratio	0,3
Thermal expansion coefficient	1,17*10^{-5} 1/°C
Wall thickness	22 mm
Outside diameter	1020 mm
Internal pressure	13 MPa
Temperature difference	45°C

During operation the pipeline will withstand some stresses associated with outer and inlet pressures, thermal expansion effect and other. In order to avoid these failures, it is necessary to check if the wall thickness is sufficient. For this task simplified criterion of Allowable Stress Design (ASD) will be applied (Karunakaran, 2018).

The next stress condition must be satisfied for the ASD check:

$$\sigma_e \leq \eta_1 * \sigma_y;$$

$$\sigma_e = \sqrt{\sigma_l^2 + \sigma_h^2 - \sigma_l * \sigma_h + 3 * \tau}$$

$$\sigma_h = \frac{p_i * D_i - p_e D_o}{2 * t} = 276,5 \ MPa$$

Where external pressure is water column pressure (p_e=0, 51 MPa at 50m depth)

In calculations, tangential stresses are assumed to be zero. Longitudinal stress is calculated as combined stress from thermal and pressure effect.

$$\sigma_l = -\alpha * E * \Delta T + v * \sigma_h = -1,17 * 10^{-5} * 2,07 * 10^{11} * 45 + 0,3 * 276,5 * 10^6$$
$$= -26 \ MPa$$

$$\sigma_e = \sqrt{\sigma_l^2 + \sigma_h^2 - \sigma_l * \sigma_h} = 290,4 \ MPa$$

$$290,4 \leq 0,85 * 414; \ 290,4 \leq 331,2$$

According to calculations, wall thickness is sufficient. The pipeline with given wall

thickness and diameter can allow the control of stresses appearing in terms of internal and external pressures. Wall thickness design is essential for pipeline installation in order to ensure the troubleproof pipeline operation during its entire lifecycle. Also, given wall thickness takes into consideration corrosion allowance. Below the scheme of wall thickness design is presented (Figure 19). Coating application, vertical and lateral on-bottom stability will be discussed in another chapter.
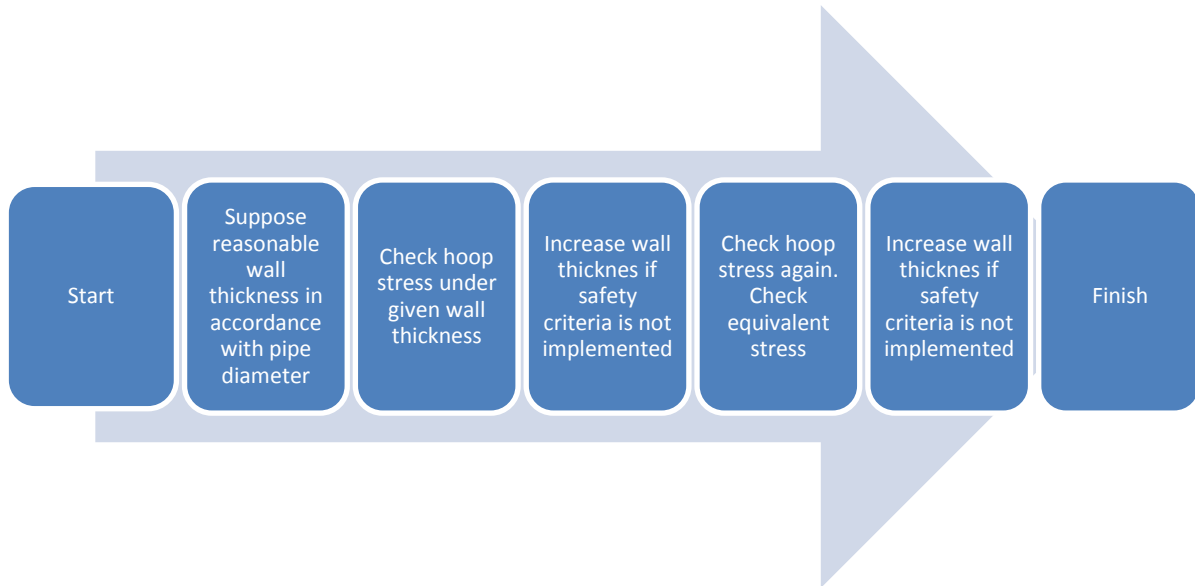
| Start | Suppose reasonable wall thickness in accordance with pipe diameter | Check hoop stress under given wall thickness | Increase wall thicknes if safety criteria is not implemented | Check hoop stress again. Check equivalent stress | Increase wall thicknes if safety criteria is not implemented | Finish |

Figure 19 – Wall thickness design methodology

Besides stresses induced by internal and external pressure, one possible issue during pipeline design may be buckling. Further buckling description is represented.

Compressive axial loads are caused in pipelines because of changes in the temperature and the internal pressure of the pipeline (Karunakaran, 2018). The buckling process may appear as an upward movement from the seabed or as lateral movements along the seabed. A conjunction of the two forms, i.e. upheaval in combination with lateral buckling, may also occur (Karunakaran, 2018). When a buckling process occur for pipelines, control of local and global buckling is necessary to be performed. Global buckling comprises a significant length of the pipeline without big deformations of the cross-section area. Global buckling is a load response and it is not a failure case (Karunakaran, 2018). It is caused by compressive axial force. The compressive axial force usually occurs because of operational temperature and pressure, which are usually above the ambient ones. Consequently, the pipeline tends to expand, but when the pipeline is constrained and not free to expand, the pipeline will get axial compressive force. While operating at higher temperatures, buckling probability rises up. Pipelines with big effective axial compressive forces and pipelines having low buckling capacity, are particularly subjected to potential global buckling. The global buckling behaviour depends on the pipe-soil interaction in high degree. This interaction comprises main uncertainties regarding

characterization as well as variation along the route, and is the most vital aspect of global buckling or expansion design (DNV, 2007). Even though global buckling is not a failure mode itself, it may, however, give rise to ultimate failure modes, such as (DNV, 2007):

- Local Buckling;
- Fracture;
- Fatigue.

Local buckling regime is limited to a short length of the pipeline exposed to substantial deformation of the cross-section area. Pipelines which tend to involve combined pressure, axial force and bending might be subjected to local buckling. Local buckling implies large deformation of the cross-section area, and operates with the following criteria to be fulfilled:

• System Collapse;

• Propagation Buckling;

• Combined load criteria.

For avoiding of buckling phenomenon, a lot of different techniques are proposed. They are trenching, burial, rock damping and others. At the same time different methods exist to control and mitigate lateral buckling in controlled manner.

Snake lay method. The Snake-lay method is a technique for buckle initiation where the pipeline is laid on seafloor in a series of smooth curves (Figure 20). The key parameters in the snake lay configuration are snake pitch, offset and the bend radius. The buckle response is influenced by the arc length which is defined by the offset and bend radius of the snake configuration. The main intent of the snake lay method is to develop a lateral buckle at some point on the curve by aiming the bend radius to be as a buckle initiator (Tewolde, 2017).
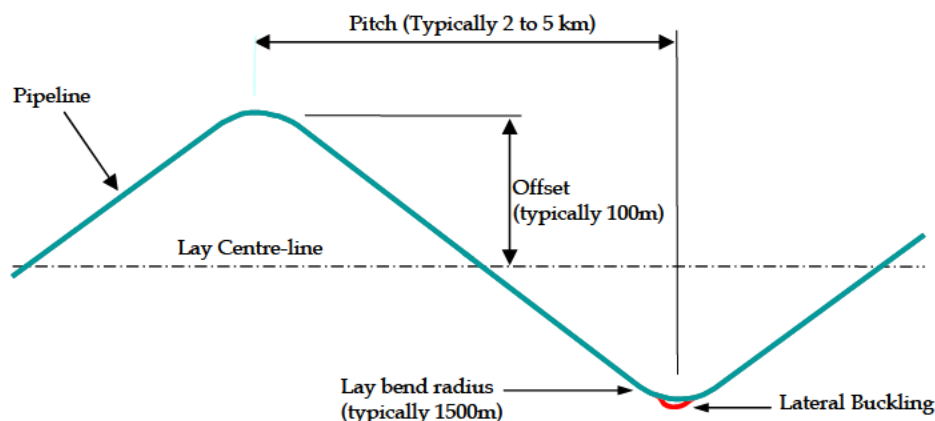

Figure 20 – Snake lay method (<u>Buckling mitigation</u>)

Vertical upset method. The vertical upset method works by specially installed vertical objects which give curvature parts along pipeline (Figure 21). The method considers that pipeline may buckle in vertical or lateral direction. Due to the irregularity of seafloor, the pipeline tends to

have lateral buckling at greater extent. Sleepers, concrete constructions or rock berms are used to create the artificial irregularities of seafloor. It is necessary to avoid very high rise of pipeline in order to get away free-span areas (Tewolde, 2017).
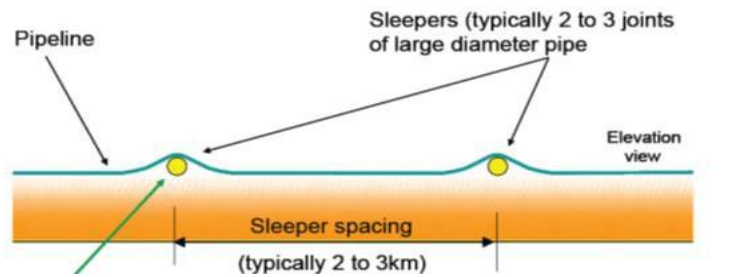

Figure 21 – Vertical upset method (Buckling mitigation)

Distributed buoyancy. In the distributed buoyancy method, buoyancy modules are fixed at pipeline each 60-100 meters in order to reduce weight. Typical buckle spacing in this method is 2 to 3km. The purpose of the buoyancy modules is to reduce the operational pipeline submerged weight to about 10% of the normal submerged weight. By installing distributed buoyance modules connected with the hydrodynamic forces create a natural out-of-straightness at the defined location. Moreover, since the submerged weight becomes lower, the lateral frictional restraint is decreased. It results in the fact, that the buckle initiation force is also reduced. The pipeline is likely to buckle at the place where the buoyance modules are applied (Tewolde, 2017).
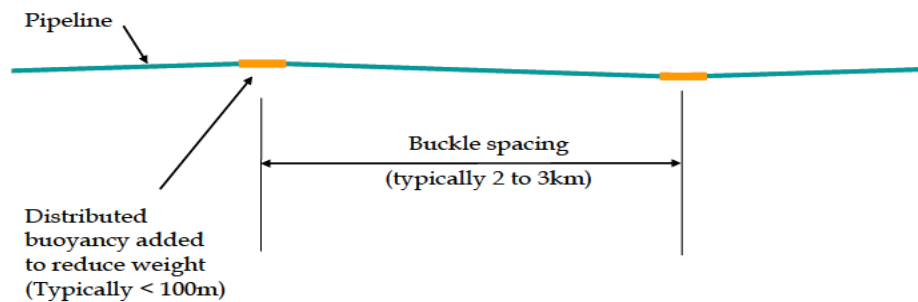

Figure 22 – Distributed buoyancy modules (Buckling mitigation)

3.3. Pipeline installation method

In this chapter, pipeline installation technique is considered. In accordance with shallow and intermediate waters, pipelaying vessel for S-Lay method may be applied as the most appropriate method compared with reel lay and J-Lay.

Solid example of such ship can be Seven Borealis vessel from Subsea 7. It has pipelaying capacity for big inch pipelines and can operate in soft ice conditions. For the Kara Sea environment operating period lasts approximately 3-4 months. Further S-Lay method is described more detailed.

S-lay is the pipeline installation methods which has S-shape curve during laying to the seabed. Before pipelaying to the seabed, the pipelines are stored, prepared and connected on the PLV (pipelaying vessel). The pipes are lowered from the vessel at the aft section through an inclined ramp (see Figure 23). The stinger is situated at the ending of the ramp. It is necessary to support the pipelines, to manage the curvature, and to avert massive deviations in the overbend region. With the defined angle, segments of the stinger can be put such way to designate its shape. Stinger length depends on two main factors such as the depth of water and pipeline submerged weight. The stinger should have sufficient length to eliminate superfluous bending which may lead to the buckling of pipeline. Tensioners are placed on the ramp and their function is to apply a force to the pipe near the stern end of the ramp (Bai, 2005).
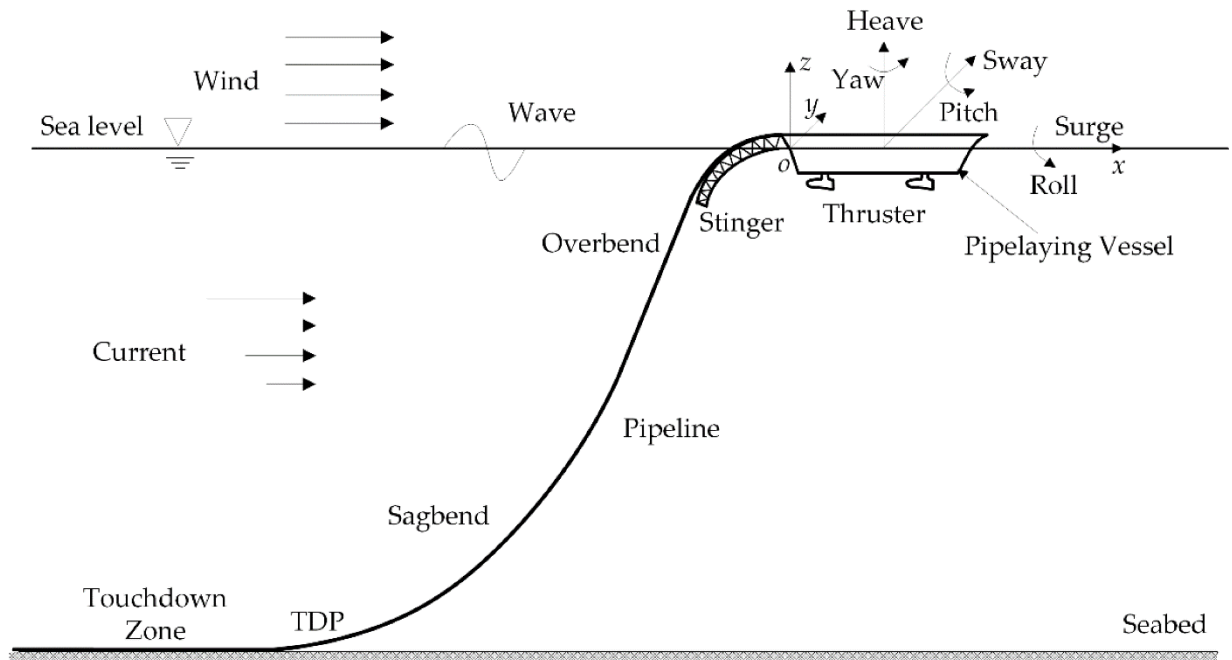

Figure 23 – Schematic S-Lay vessel (Xu et al., 2018)

The top curved section of pipeline is called the "overbend" (Kyriakides et al, 2007). The pipeline will move down straight, then little by little it will bend in the opposite way known as the sagbend region. From the sagbend region, the hanged pipeline intends to reach the seafloor at

the touchdown point. The detailed scheme of the S-Lay configuration is represented in Figure 24. In the sagbend region, the conjunction of bending and pressure loads should be supported in safe way to avoid any failures (Kyriakides et al, 2007). The tension applied at the upper side is utilized to control the curvature line in the sagbend area. Superfluous bending, local buckling and other fault case might happen if the top tension is missed due to sudden vessel movements. The major goal of PLV is to provide tension for the keeping of hanged pipeline sections and to regulate their shape.
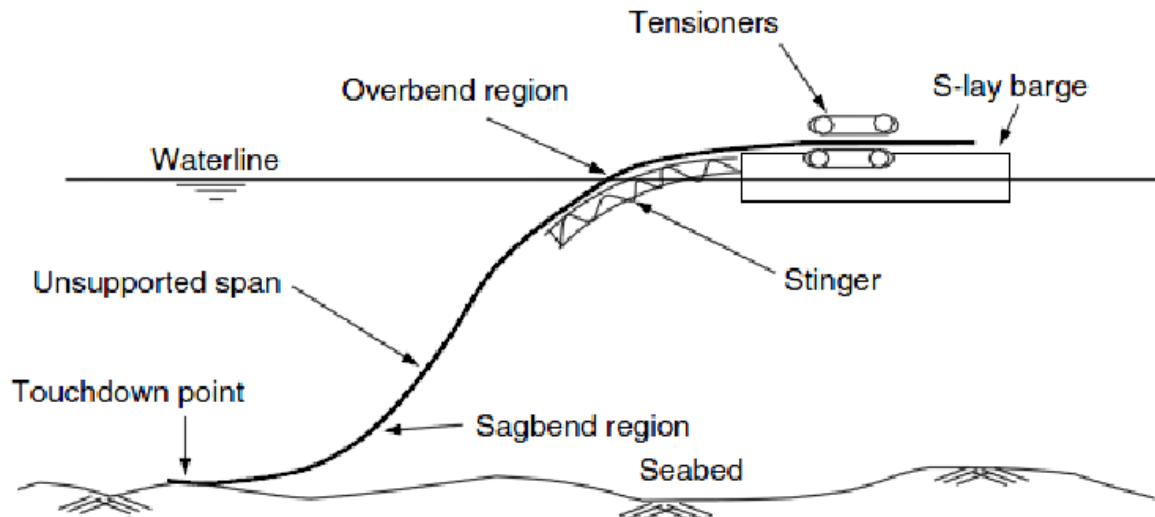
Figure 24 – Pipeline configuration during S-Lay method (Bai, 2001)

The crucial factors during installation are:

• To get away buckling faults in the overbend and the sagbend regions;

• To ensure the elastic regime for the pipeline. If plastic deformation is present on the overbend or sagbend, it may lead to the process of ovalization and torsion of the pipeline on the seafloor (Karunakaran, 2018).

S-Lay method comprises some aspects which should be considered with some degree of importance. They are the allowable strain in the overbend area and the permissible bending moments in the sagbend area. Tensioning capacity, stinger length and radius and longitudinal trim of the ship are regulated by water depth where pipeline is planning to be laid (Bai, 2005).

Generally, S-Lay method is performed by the following major installation devices:

Stinger. The stinger is an extension over board the stern of an offshore pipe lay barge used to provide additional support pipeline by the creation of curvature at the overbend region during offshore construction process (Jaeyoung, 2007). Typically, hinged members are located in the stinger for the stinger curvature adjustment. The vast types of ships possess the various lengths of stinger and for installation in shallow water area the length shouldn't be more than 100 meters. Applying very short stinger, there is possible higher bending with consequent pipeline crash during installation process. The stinger should have ability to withstand different loads

which act during operation (Perinet et al., 2007):

- Hydrodynamic loads due to waves, currents and wind load;
- Pipeline self-weight load;
- The stinger self-weight.

There are two kinds of stinger types for nowadays:

- Rigid stinger

This kind of stinger has rigidly fixed outline with determined length and a non-regulating curvature angle. The stinger is set tightly at the vessel and it restricts wide movements.

- Articulated stinger joined by hinges

The kind of stinger which can regulate curvature angle thanks to the assembly of hinges in each segment. It is possible to set the angle approximately equal to vertical line. This configuration permit to decrease stresses in pipelines due to free span length in conditions of deep-water regions.

Tensioners. Tensioners are usually situated close to the ship aft. The friction between rubber strips in the tensioning mechanism transmits a tension on the pipeline to regulate the curvature line during pipelaying process and to ensure the pipe integrity. The needed tension depends on water depth, stinger radius and length, pipe size and its weight. The required tension increases while weight, water depth and length rise up. The installation ship tension capacity governs a limitation for pipelaying depth (Jaeyoung, 2007).

Utilizing S-Lay method, the pipeline doesn't contact directly to the stinger but it has interaction with some rollers. Because of this the friction force between the pipeline and the stinger is reduced.
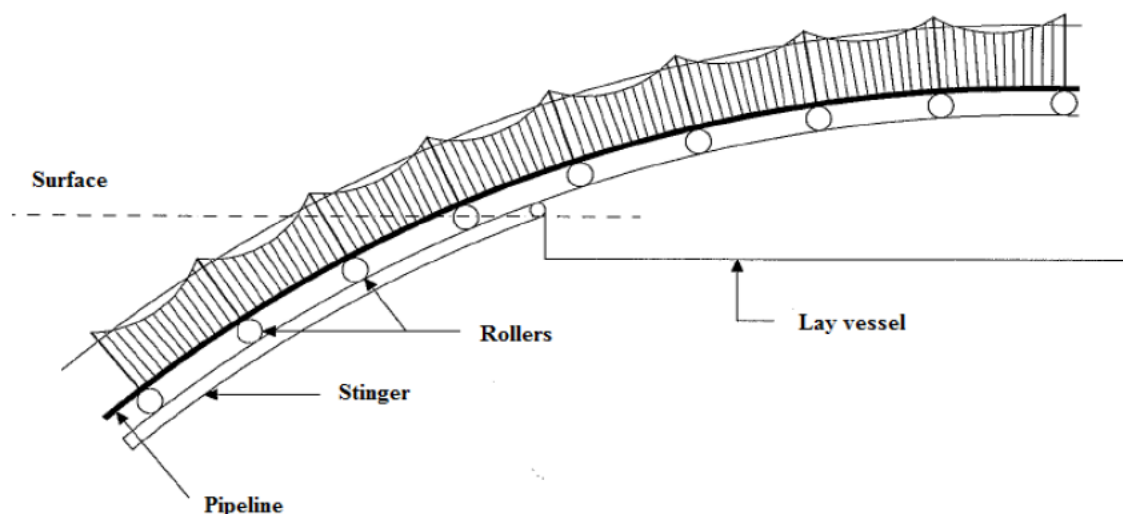

Figure 25 – The pipeline rests on rollers (Tewolde, 2017)

The process of pipeline installation by S-Lay method can be divided for next steps:

- The vessel is fixed at chosen location by a mooring system (or DP);
- The pipes are delivered to welding station (firing zone) for technological purposes;
- Tensioners apply a force to the pipe near the aft end of the ramp;
- The welded and coated pipes supported by the stinger, then get away from PLV;
- The form of the pipeline in the sagbend region is controlled by the interaction between the applied tension and pipeline submerged weight.

S-Lay method surely has high priority in Kara sea condition. There are some advantages (Karunakaran, 2018):

- High pipelaying rate: 3-7 km/day (very important due to short weather window in the Kara Sea);
- Wide range of diameters: up to 60" OD (possible to lay coated pipes);
- Long vessels with large pipe storage capacities;
- Very suitable for given water depth (up to 100 m).

3.4. Pipeline route

Offshore field development includes installation of oil and gas pipelines on the seabed. Pipeline routing is a technical engineering approach for connecting to points by pipeline with minimum cost and minimum pressure drop. For Pobeda field there are four possible routes:

1. Pobeda-Belushya Guba pipeline through Novozemelsky trench (465 km);
2. Pobeda-Belushya Guba pipeline bypassing Novozemelsky trench (680km);
3. Pobeda pipeline to Yamal peninsula (420 km);
4. Pobeda to Yamal peninsula (645 km).

Each pipeline route has its own features. Figure 26 and figure 27 show different routes from Pobeda field to onshore bases and seabed profiles. Of key importance is the depth profile along the pipeline route. The expected maximum draft of drifting icebergs is assumed to be 77m as discussed previously.
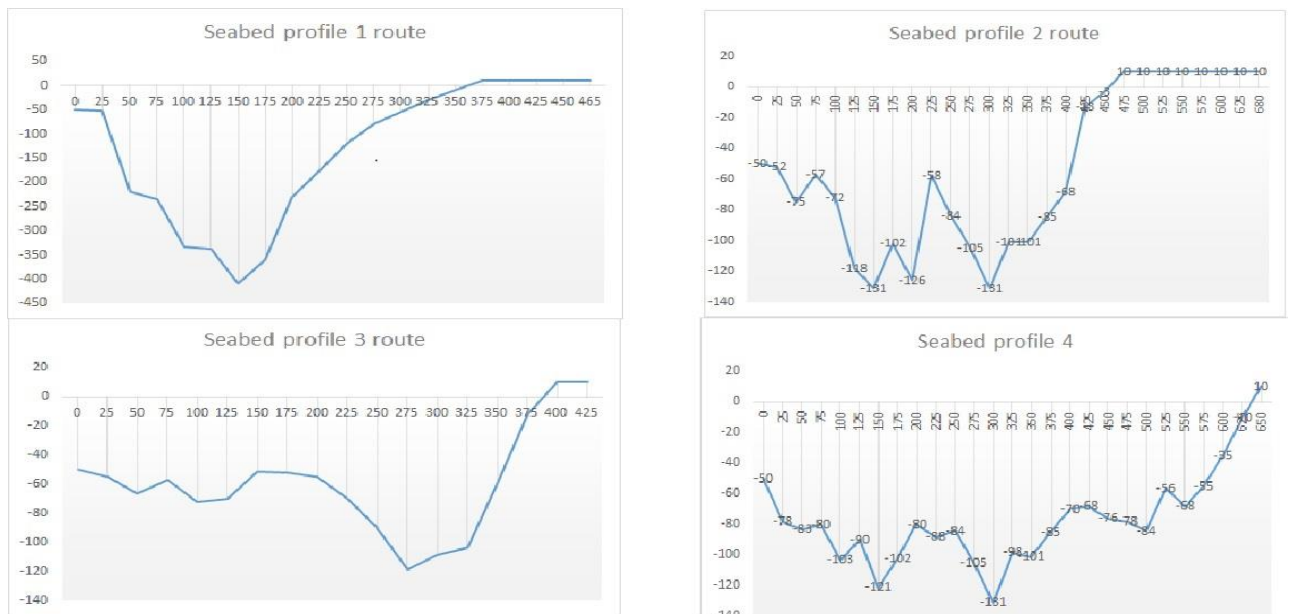

Figure 26 – The sketch of different routes

Figure 27 – Seabed profiles

In order to choose the most economical and efficient pipeline route, a cost map is present in Figure 28. Discrete cost map is driven by geotechnical surveys, GIS data (ice conditions, water conditions) and analyses.
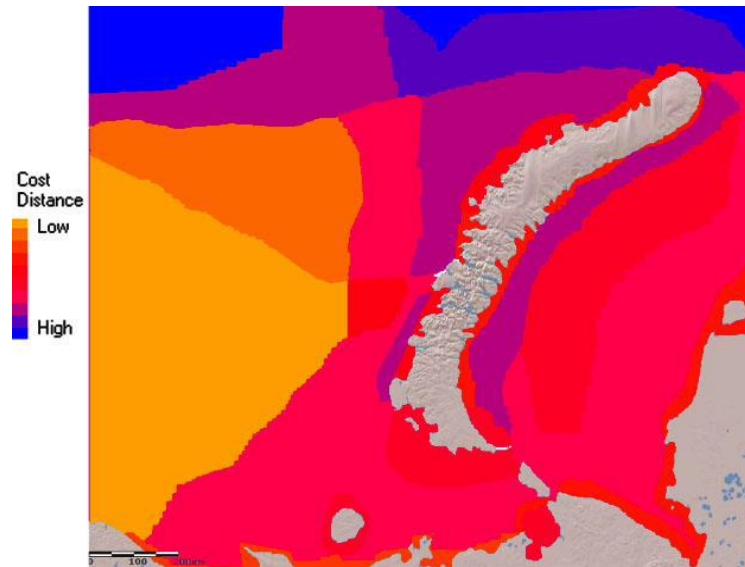

Figure 28 – Cost map (Starodubtcev, 2016)

In accordance with cost map, the pipeline installation through Novozemelsky trench requires high investments due to deep-water region. The second route affords to avoid deep-water zone, but the route length and installation costs are higher compared to the third variant of route. Moreover, there are no infrastructure or gas facilities at Belushya Guba. The construction of technological complexes is suitable only in case of development of several gas fields (Shtokman field, for instance) and a robust customer market. The table 13 gives comparison between pipeline routes.

Table 13 – The comparison of different routes

Tag \ Route	1st variant	2nd variant	3rd variant	4th variant
Water depth	Deep-water region	Shallow water	Shallow water	Deeper water
The length route	Moderate length	High length	Moderate length	High length
Technological facilities	No technological complexes	No technological complexes	Yamal LNG, Bovanenkovo-Ukhta pipeline	Yamal LNG, Bovanenkovo-Ukhta pipeline

The fourth variant of pipeline route (Figure 29) is subjected to be the most efficient due to the presence of existing technological facilities and avoiding grounded icebergs, in spite of high installation cost due to long route. Moreover, deeper waters offer to avoid drifting icebergs with maximum draft. The main disadvantage of previous variants is no existing technological complexes for gas processing. Therefore, it requires huge investments for design and construction and it is not relevant for the only field.

Figure 29 – Possible pipeline routing between Pobeda field and onshore facility

For the Kara Sea region pipeline route is challenge due to serious weather conditions and uneven seabed. However, the main advantage of curved pipelaying is avoiding dangerous areas with grounded icebergs. Curved pipelaying method affords to keep pipeline in safe manner and this method prevents from accidents, namely a collision of pipeline with iceberg.

Besides, at chosen pipeline route the main issues are associated with natural seabed

obstacles. Good example of such irregularity is a round-shape hillock (Figure 30). These hillocks can reach up to 400 meters in diameter and 2-5 meters in height. There are several hillocks during pipeline route (AARI, 2017). To overcome such obstacle, the curved pipelaying method can be applied. This method affords to get around hillock and to keep pipeline in reliable manner.
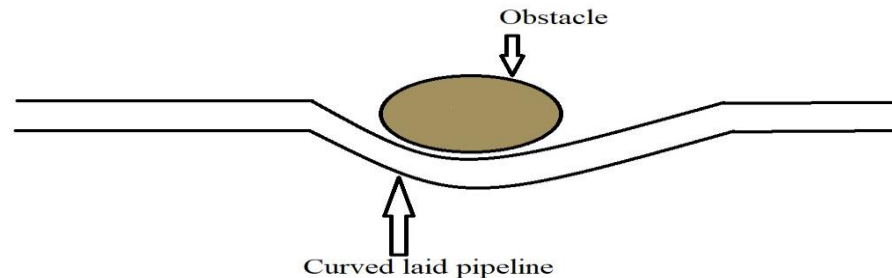

Figure 30 – The sketch of curved laid pipeline

To perform the chosen configuration in a curved route, a sufficient lateral force created by pipeline-soil interaction should be provided (Karunakaran, 2018). The lateral force is some function of pipeline submerged weight, soil properties, contact length and others. In other words, successful curved laying should be defined by robust pipeline on-bottom stability.

Pipeline on-bottom stability is a sophisticated interaction between the hydrodynamic loads, the pipeline shape and the surrounding soil. The pipeline length can alter from several meters up to hundreds of kilometres. For a long pipeline route, it is more likely that one or more of the water depths, the pipeline heading, the metocean conditions or the soil conditions will vary. The major document which takes into account all aspects about pipeline on-bottom stability is (DNV, 2010). In accordance with this standard, there are two types of stability such as vertical and lateral. Vertical stability should be considered to avoid floating or sinking of the pipeline. This type of on-bottom stability is not complicated and appropriate calculations for given pipeline will be shown later. In turn of lateral pipeline on-bottom stability, it can be divided for 3 groups (Bassem et al., 2017):

1. *Absolute stability method*

The Absolute Stability method is performed to ensure the minimum pipe submerged weight such way that no lateral displacement occurs during the design storm return period. This method is 2D method and comprises force equations equilibrium for parameter calculations. The method utilizes the maximum wave velocity expected during the entire storm period. Thus, the pipeline submerged weight estimated tends to be very conservative (Bassem et al., 2017).

There are some remarks and limitations of the method:

- This method is based on the extreme wave velocity which might occur for a few seconds during the three hours storm period at one particular location along the whole pipeline route;
- The method does not take into account operational temperature and pressure for the pipe.

2. *Generalized stability method*

The generalized stability method is based on the large number of dynamic stability analyses of 2D pipeline. The method considers pipeline lateral displacement in a range from 0.5 diameter to 10 diameters under design storm return period loading conditions. The dimensionless lateral pipe displacement (Y) is governed by a set of non-dimensional parameters (DNV, 2010):

$$Y = f(L, K, M, N, \tau, G_s, G_c)$$

There are some limitations of this method (Bassem, 2017):

- This method is based on 2D section of the pipeline and it disregards the benefits of 3D effect on the pipeline bending and axial stiffness and soil resistance on the pipeline stability;
- Unlike the Absolute stability method, this method utilizes the significant wave velocity to evaluate the pipeline submerged weight values corresponding to pipeline lateral displacement in range between 0.5 outer diameter (OD) and 10 OD;
- Similar to the Absolute stability method, the method does not take into consideration the pipeline operational temperature and pressure;
- The method is applicable for silica sand soil and clay soil only and cannot be used for other soil types (carbonate sand soils).

3. *Dynamic stability method*

The dynamic stability method is considered as the most complicated stability method because it requires a numerical modelling software and a level of experience to implement the modelling and interpret the results. Using the finite element analysis for modelling, the limitations of 2D methods are overcome. The following considerations are required for the dynamic stability design by DNV document (Bassem, 2017):

- Complete sea-state time series using the wave spectrum should be used in the model; in case there is no information about it, a typical storm period of three hours may be used;
- Storm hydrodynamic loads of irregular wave should be computed utilizing advanced hydrodynamic force model (wave wake effect accounting);

- There is the simulation time history for hydrodynamic loads in this method;

- Soil resistance consists of two parts such as pure friction part and a passive resistance term, considering the pipeline penetration in the soil and build-up of the soil berm;

- For modelling full pipeline length is considered. If the pipeline length is long enough, it is possible to model a particular section with defined boundary conditions;

- The operating temperature and pressure can be included in the model.

There are some limitations of this method (Bassem, 2017):

- There should be included a different number of pipeline properties for more accurate modelling such as axial stiffness and bending stiffness, nonlinear cross section properties and others;

- For small diameter pipelines, DNV standard does not ensure any considerations regarding the wave velocity and hydrodynamic load corrections. Thus, the results of the 2D stability methods and dynamic method can be differ a lot if the wave velocity and the hydrodynamic loads are not correlated.
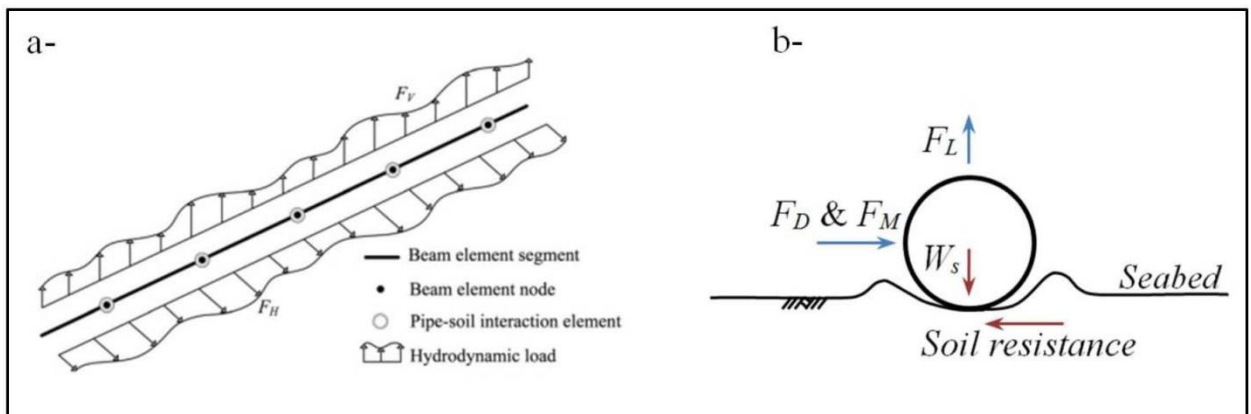

Figure 31 – The sketch of hydrodynamic pipeline-soil model elements (Bassem, 2017)

For the considered case in this master thesis when pipeline is laid in curve, next condition should be implemented (DNV, 2010):

$$H \leq R_c * (\mu_s * w_s + F_R)$$

This condition is present in order to avoid that the curved pipe slides in the radial direction. In accordance with (DNV, 2010), hydrodynamic forces can be neglected in this assessment.

The basics of pipeline-soil interaction aspect

Different aspects of subsea pipeline design are influenced by geotechnical reasons and the expected pipeline-soil interaction response such as (White et al, 2017):

- Route selection;

- In-place stresses after pipeline laying, due to irregularities of the seabed (bottom roughness);
- On-bottom stability of pipelines under wave and current loading;
- Pipeline responses to temperature and pressure induced loading.

One of the most crucial parts of the on-bottom stability dynamic analysis is to consider the full soil resistance which consists of a pure Coulomb friction part (μ) and a passive resistance part (F_R). The Coulomb friction value ensures the lateral soil resistance capacity as a ratio of the pipeline vertical weight. (DNV, 2010) has got different friction values for a concrete coated pipeline depending on the soil type. The passive soil resistance part takes into consideration the soil resistance capacity due to pipeline penetration into seabed.

Considering only pure Coulomb friction term and disregarding the passive soil resistance term during on-bottom stability modelling may lead to bigger pipeline horizontal displacements.
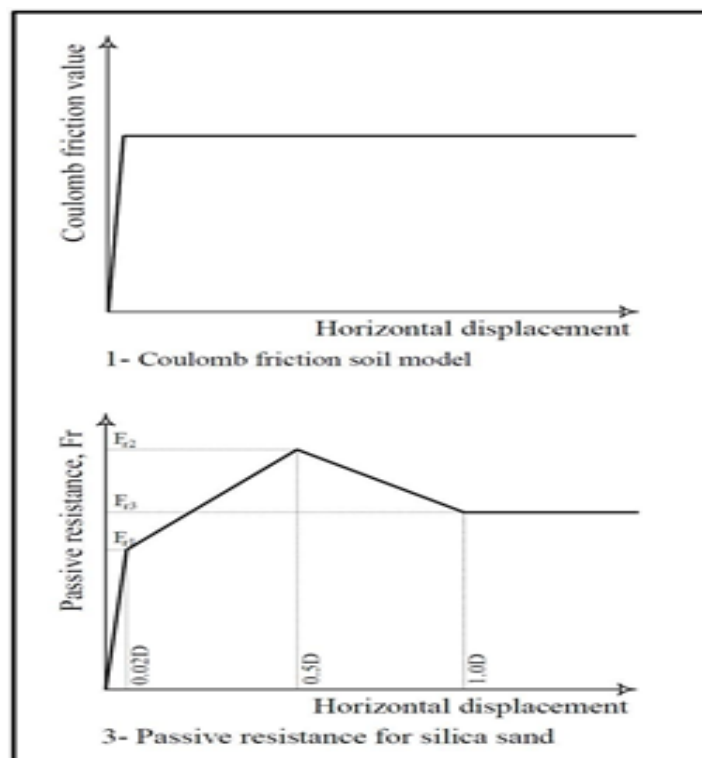

Figure 32 – Two terms of friction (White et al, 2017)

The major pipe-soil interaction parameters are the limiting resistances during axial or lateral pipe movement (for both buried and on-bottom laid pipelines). There are different models with increasing complexity how to estimate pipe-soil interaction (White et al, 2017):

- A single limiting value of axial or lateral resistance (or friction factor) – a rigid-plastic response;
- An independent force-displacement response (non-linear 'springs');
- A general vertical-lateral response model;

- Explicit modelling of the soil continuum, pipe and pipe-soil interface.

In frame of this master thesis, the simplest pipe-soil interaction (as a single value) is considered because more detailed investigation of this aspect is necessary for the deep-water pipelines, in particular the problems posed by high pressure, high temperature (HPHT) pipelines. Moreover, the research of pipe-soil interaction is not the aim of given master thesis.

Calculation of on-bottom stability

As it was discussed earlier, for curved laid pipeline vertical stability should be ensured against floating. In order to check vertical pipeline on-bottom stability (DNV, 2010) can be utilized. According to this document, the submerged weight of the pipeline shall meet the following criterion (DNV, 2010):

$$\gamma_W * \frac{b}{w_S + b} \leq 1, where\ \gamma_W\ (safety\ factor) = 1,1;\ b\ (buoyancy\ force)$$

Knowing pipeline parameters without coating, w_d can be calculated.

Table 14 – Pipeline parameters with no coating

Parameters	Values
Steel density	7850 kg/m^3
Polyethylene corrosion protection	4 mm
Polyethylene density	980 kg/m^3
Pipeline diameter: D_o and D_i	1020 mm and 976 mm
Sea water density	1025 kg/m^3

$$w_d = \rho_s * \pi/4 * (D_0^2 - D_i^2) * g + \rho_p * \pi/4 * (D_{01}^2 - D_0^2) * g = 5446 + 127 = 5572\ N/m$$
$$b = \rho_w * g * \pi * \frac{D_{01}^2}{4} = 8557\ N/m$$

Obviously that DNV requirement is not fulfilled, so concrete coating is necessary to make pipeline heavier and to provide vertical stability. In accordance with (DNV, 2017) concreate thickness 60 mm (3000 kg/m^3) is taken.

$$w_d = \rho_s * \frac{\pi}{4} * (D_0^2 - D_i^2) * g + \rho_p * \frac{\pi}{4} * (D_{01}^2 - D_0^2) * g + \rho_c * \frac{\pi}{4} * (D_{02}^2 - D_{01}^2) * g = 11693$$

$$b = \rho_w * g * \pi * (\frac{D_{02}^2}{4}) = 10610\ N/m$$

$$\gamma_W * \frac{b}{w_S + b} = 1,1 * \frac{10610}{1083 + 10610} = 0,99 \leq 1$$

Now requirement of (DNV, 2010) is fulfilled and pipeline will not float after installation at the seabed.

Next step is to check lateral on-bottom stability. Lateral stability is necessary in order to avoid significant lateral displacements of pipeline. For calculations permanent conditions are taken into account, namely the 10-year return condition for waves combined with the 100-year return condition for current. The water depth is taken like an average value during pipeline route.

Initial data is present in table 15.

Table 15 – Initial data for lateral on-bottom stability calculation

Parameter	Value
Depth, d	80 m
Significant wave height, H_s	6,2 m
Peak period, T_p	12,5 sec
Outside diameter of pipeline, D	1,148 m
Current velocity at 40 m above seabed, U_r	0, 78 m/s
Seabed roughness, z_0	$5*10^{-6}$ m
Angle for waves and currents, θ	90º

From (DNV, 2010) the wave parameter, T_n can be found as:

$$T_n = \sqrt{\frac{d}{g}} = 2,83 \sec and \frac{T_n}{T_p} = 0,23$$

In accordance with (DNV, 2010) peakedness value is found: $\varphi = \frac{T_p}{\sqrt{H_s}} = 5,01; \gamma = 1$

Using figure in (DNV, 2010) U_s can be found as: $\frac{U_s*T_n}{H_s} = 0,14; U_s = 0,31 m/s$

Also, the ratio T_u/T_p and T_u have values: $\frac{T_u}{T_p} = 1,07; T_u = 13,4 sec$

As $\frac{T_n}{T_u} > 0,2 consequently T^* = 1 * T_u = 13,4 sec$

The number of waves in storm equals: $\tau = \frac{T_{storm}}{T_u} = \frac{3*3600}{13,4} = 806$

The oscillatory velocity amplitude for single design oscillation U^*:

$$U^* = 0,5 * \left(\sqrt{2ln\tau} + \frac{0.5772}{\sqrt{2ln\tau}}\right) * U_s * R_D$$

Where, R_D is taken 0,95 for Kara Sea as discussed value. Consequently, U^*=0,56 m/s

The mean perpendicular current over the pipe diameter is taken according to (DNV, 2010):

$$U_c(z_0) = U_r(z_r) * \left(\frac{\left(1+\frac{z_0}{D}\right) * \ln\left(\frac{D}{z_0}+1\right) - 1}{\ln\left(\frac{z_r}{z_0}+1\right)}\right) * \sin\theta; U_c = V^* = 0,56 m/s$$

Keulegan-Carpenter number for single design oscillation (K^*) and steady to oscillatory velocity for single design oscillation (M^*) have values 6,5 and 1 respectively.

Hence from graph in (DNV, 2010) peak load coefficients are: $C_Y^* = 2,14; C_z^* = 1,18$

In accordance with the type of soil and discussions with Subsea 7 specialists about this issue total penetration (z_p) and soil friction (μ) are taken 0,2 meters and 0,35 respectively. Hence, load

reductions factors are: $r_{tot,z} = 0.7 * 1 * 0.9 = 0.63; r_{tot,y} = 0.76 * 1 = 0.76$.

The peak horizontal load is: $F_Y^* = C_Y^* * r_{tot,y} * \rho_w * 0.5 * D * (U^* + V^*)^2; F_Y^* = 1200 \, N/m$

The peak vertical load is: $F_z^* = C_z^* * r_{tot,z} * \rho_w * 0.5 * D * (U^* + V^*)^2; F_z^* = 549 \, N/m$

For the calculation of passive soil resistance (DNV, 2017) was applied. The soil data is below:

Table 16 – Soil data (AARI, 2017)

Parameter	Value
Soil dry weight, γ_S	17 kN/m^3
Undrained shear strength, S_u	40 kPa

F_c is the difference between submerged weight and vertical force: $F_C = W_s - F_Z^* = 534 \, N/m$

According to (DNV, 2017) there are two non-dimensional coefficients for clay soil:

$$G_C = \frac{S_u}{\gamma_s * D} = 2.05; k_C = \frac{S_u * D}{F_C} = 86$$

Hence, $\frac{F_R}{F_C} = \frac{4.1 * k_C}{G_C^{0.39}} * \left(\frac{z_p}{D}\right)^{1.31} = 27; F_R = 14418 \, N/m$

The pipeline is considered to satisfy the absolute stability requirement if:

$$\gamma_{SC} * \frac{F_Y^* + \mu * F_Z^*}{\mu * w_S + F_R} \leq 1 \text{ and } \gamma_{sc} * \frac{F_Z^*}{w_S} \leq 1$$

During discussion in Subsea 7 and with specialists in Rosneft company, safety criteria (γ_{SC}) for Kara sea is taken with value 1,83. Thus, the resulting values are: $0.17 \leq 1 \text{ and } 0.93 \leq 1$. Both equations satisfy the absolute lateral stability criteria. Hence, the horizontal stability criterion shows that pipeline is stable.

In accordance with (Jaeyoung, 2007), curved pipeline route consists of three section such as two straight sections and one curved section between formers. The major challenge for curved laying pipeline is to ensure sufficient lateral stability, avoiding slippage during installation and further pipeline operation. Generally, required minimum pipeline route curve radius should be defined to prevent slippage effect on the seabed. Typically, without penetration for given pipeline (D_o=1148mm) sufficient radius R_c is more than 1000m (Karunakaran, 2018).

Obviously, this radius is big enough, so it leads to long straight sections too. In turn, long straight sections and large radius make install turnpoints during pipeline route in order to facilitate steep curves (Karunakaran, 2018). Turnpoints installation requires extra expenditures and leads to higher project cost. At the same time installation experience shows that curves reported to be unstable, actually are stable.

Moreover, the Kara Sea seabed is considered to be uneven with different ground imperfections and traditional primitive method may be under-conservative. To overcome some challenges in curve laid pipeline routing SIMLA software is applied in this master thesis.

3.5. The basics of SIMLA software

This chapter gives the main theory and necessary statement about SIMLA software. The base of this software is finite element method. The finite element method is a commonly used numerical method, which is utilized to solve problems associated with stress analysis, fluid dynamic and heat transfer problems. In this chapter the major significance will be on the non-linear finite element method and the nonlinearities which are used in structural analysis.

The finite element method has got the same foundation as structural analysis in overall, where the following principles apply for both linear and nonlinear element method:

1. Equilibrium;
2. Stress-strain relationship;
3. Kinematic compatibility.

Equilibrium. Equilibrium is the first of all three principles that structural analysis is based on. Structure equilibrium is signified by means of the Principle of Virtual Displacements (Sævik, 2008). It asserts that the work performed by the true internal stresses and external forces equals each other when the structure is subjected to a virtual displacement field that fulfils the boundary conditions. Instead of trying to find the exact solution, the principle introduces approximate functions and intends to in average fulfil the differential equation for the problem using weight functions and volume integration (Sævik, 2008). Choosing weight functions such that the corresponding boundary conditions are fulfilled, one can get a condition where the error in average for the total volume of integration is zero. However, the differential equation is not compulsory realized at an arbitrary point within the volume. The formulation of the virtual work in SIMLA ignores volume forces, but takes into account initial stresses. The principle of virtual displacement in an arbitrary equilibrium state then reads (Sævik, 2008):

$$\int (\rho a - f)\delta u dV + \int (\sigma - \sigma_0) : \delta \varepsilon dV - \int t * \delta u dS = 0$$

Where:
- ρ is the material density;
- a is the acceleration field;
- f is the volume force factor;
- u is the displacement vector;
- σ is the stress tensor of Cauchy stress;
- σ_0 is the initial stress tensor;
- ε is the strain tensor of natural strain;
- t is the surface traction.

As a rule, most quantities are referred to the initial C_0 configuration where Green strain and 2nd Piola-Kirchoff stress are energy conjugated quantities where the 2nd Piola-Kirchoff stress tensor S is given by (Sævik, 2008):

$$S = \frac{\rho_0}{\rho} * F^{-1} * \sigma * F$$

Where:

ρ is the density in the unreformed configuration, ρ_0 is the density in the deformed configuration and F is the deformation gradient.

Stress-strain relationship. The stresses need to be related to strains. For elastic materials, this is performed in accordance with Hooke's law. When the stress achieves the proportional limit, a nonlinear relationship occurs. In this case, it is necessary to apply an elastoplastic formulation which takes into consideration both the stresses in the axial and the hoop directions of the pipe (Sævik, 2008). In order to state the basis for the plasticity and calculate the plastic strain, there are three main features:

1. A **yield condition**: It is the stress state in which plastic deformation first occurs. Different yield conditions have been assumed, but experiments showed that von Mises yield condition is the best one representing the material behaviour for most metals. The yield condition can generally be expressed as: f (S, k) =0, where f is a scalar function, k is a strain-hardening parameter that depends upon the load history in the plastic range, and S is the 2nd Piola-Kirchoff stress tensor (Sævik, 2008).

2. A **flow rule**: This rule defines the plastic strain increment and stress rate at every point in the load history. The flow theory and the deformation theory give relationship between stress and plastic strain. SIMLA is based on the flow theory, which is better for treating problems associated with cyclic and reversed loads.

3. A **hardening rule**: This rule determines the change of the yield condition as the plastic flow proceeds. The hardening is described by either isotropic or kinematic model, both included in SIMLA software. The major difference is the fact that material remembers the hardening that has occurred in the isotropic model, i.e. the yield condition is not changeable when loading is reversed.

Kinematic compatibility. Structure compatibility requirement ensures that all contiguous cross-section areas will obtain the same displacement and deformation. The material itself will remain continuous as it deforms, any cracks will not appear and the strain will be finite. In SIMLA software there is assumed that Bernoulli-Euler and Kirchoff-Navier's hypothesis apply, i.e. plane sections perpendicular to the neutral axis remains plain and perpendicular to the neutral axis after loading and consequently, there are no shear deformations (Sævik, 2008). The pipe element parameters are showed on Figure 33.
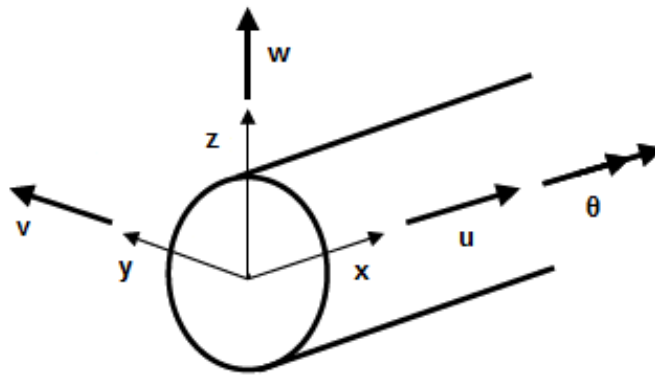
Figure 33 – Pipe element parameters (Sævik, 2008)

There are several nonlinearities in SIMLA software. Two main nonlinearities are presented in structural analysis (Sævik, 2008):

- Geometrical nonlinearities: For larger displacements, the geometry may alter and the load changes through the analyses. Geometric nonlinearities will rise up if the structure obtains deformations, consequently equilibrium equations need to be expressed with respect to the deformed configuration.

- Material nonlinearities: The material behaviour becomes nonlinear when the stress surpasses the yield limit. When the yield limit is achieved, the material curve goes to the plastic area, where the stress-strain relationship changes due to variation in the elasticity modulus, and Hook's law cannot be applied.

In SIMLA software both static and dynamic analyses can be fulfilled.

Static solution procedure is based on user defined load control with Newton-Raphson equilibrium iteration at each load step (Sævik, 2008). This method is supposed to be the most commonly used iterative method for solving non-linear structural problems. The method is illustrated in Figure 34, and the procedure utilized in SIMLA is written as (Sævik, 2008):

$$\Delta r_{k+1}^i = K_{T,k+1}^{-1i} \Delta R_{k+1}^i$$
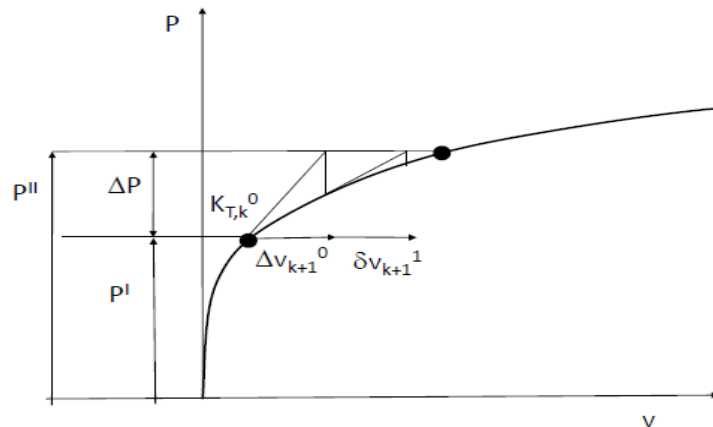
Figure 34 - Illustration of Newton-Raphson iteration (Sævik, 2008)

Dynamic solution procedure implies that nonlinear dynamic problems cannot be solved by modal superposition and therefore direct time integration of the equation of motion is necessary. This can be performed either by an explicit method or an implicit method (Sævik, 2008).

Explicit method. The method means that the displacement at the new time step, t+Δt, can be obtained by means of information at the state of the system at the current time.

$$r_{k+1} = f(\dot{r}_k, \dot{r}_{k-1}, r_k, r_{k-1} \ldots)$$

Explicit methods are conditionally stable and therefore rather little time steps must be used. If these methods are formulated in terms of lumped mass and lumped damping matrices it is not necessary to solve a coupled equation step (Sævik, 2008). Explicit methods are typically utilized in explosion and impact analysis because small time steps are applied for the achievement of good accuracy.

Implicit method. The displacements in an implicit method depend on quantities at the next time step, together with information from the current step (Sævik, 2008).

$$r_{k+1} = f(\dot{r}_{k+1}, \dot{r}_k, r_{k+1}, r_k \ldots)$$

Implicit methods definitely have better numerical stability than explicit methods, as information about the next step is used. These methods may become low cost efficient if small time steps are inevitable due to accuracy requirements. This is due to the fact that it is necessary to solve the coupled equation system at each time step (Sævik, 2008). The various implicit methods exist in connection with how the acceleration is proposed to alter between the time steps and at which time the equilibrium equation will be performed. Making assumption that there is constant average acceleration between the time steps, the result will be an unconditionally stable method, consequently this method is preferable for long-term analysis. Constant average acceleration between the time steps can be applied in SIMLA software, which utilizes the HHT-α method (Hilbert, Hughes and Taylor method), by setting the control parameter for the dynamic analysis $\beta = 1/4$. The HHT-α method damps high frequency modes and at the same time keeps 2nd order accuracy.

3.6. Simulation process in SIMLA

SIMLA is special software for engineering analysis of subsea pipelines during design, installation and operation. SIMLA software is based on the non-linear finite element method, where both static and dynamic analysis can be performed. In this thesis, SIMLA has been used during laying, where new elements are introduced from a moving vessel. The purpose of the analysis is to achieve satisfying curve stability and to introduce turnpoints if there is instability. The input data was provided by Subsea 7 Company. For pipelaying process "Seven Borealis" vessel is used. This vessel has sufficient stinger length, stinger radius and pipe range, consequently this vessel is suitable for chosen 40-inch pipeline. For modelling the optimal lay angle was found to be 36 degrees as a robust angle for shallow water.

A simple predetermined route has been investigated, consisting of two straight distances with a curved section with a radius of 350 meters. This route is built by using MATLAB software and then it is converted in txt-format file. Having created route file, the simulation program script is written and obtained results are exposed by post-processing. The input file to SIMLA is generated in FlexEdit, namely special text editor created by Marintek. After performed simulation, Xpost program can be used for visualization and Matrixplot is suitable for getting graphs and charts.
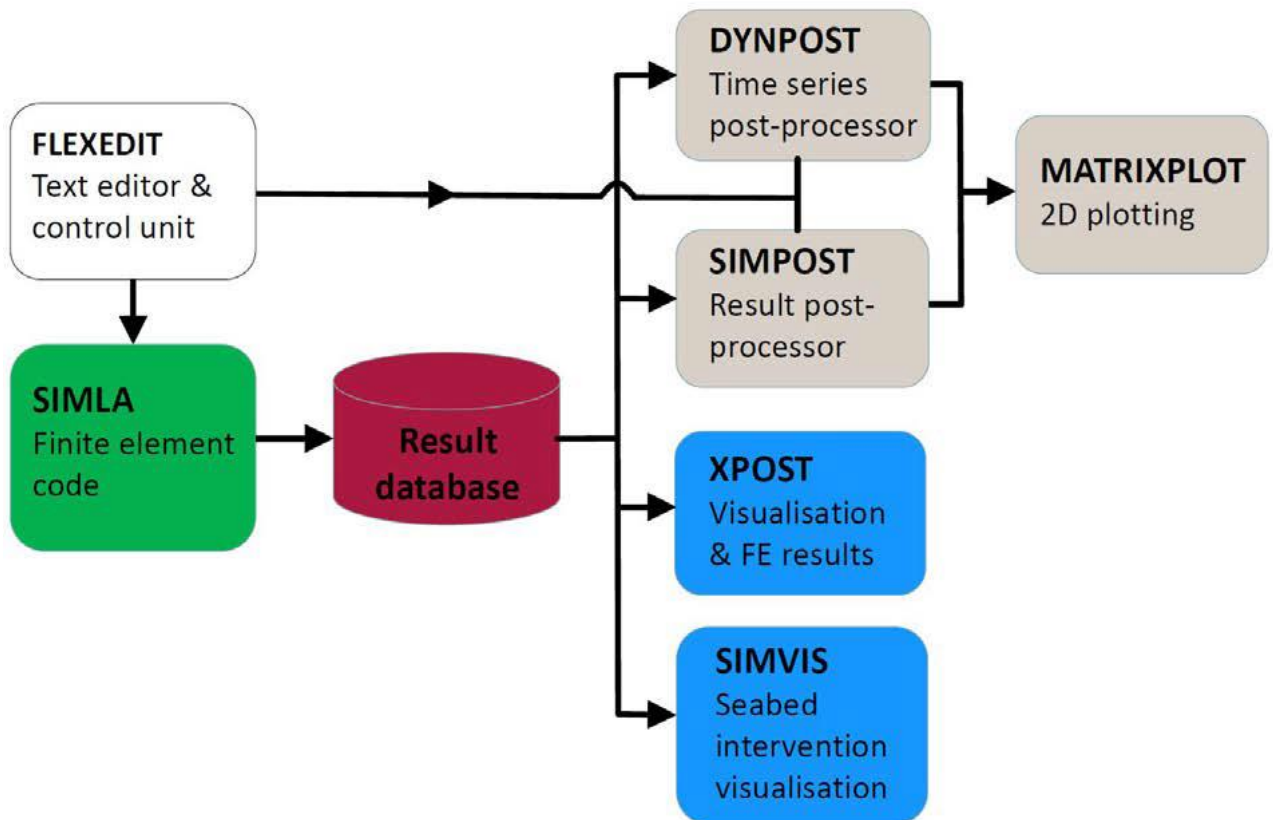
Figure 35- The interconnection between the parts of SIMLA software (Sævik, 2017)

In SIMLA software two analysis are performed; respectively static and dynamic analysis. In both cases the time domain is used to characterize the load histories and the analysis order. The order of analysis is controlled by the TIMECO card, which determines a set of time intervals where different properties may apply with respect to step length, time interval for restart info and result storage and type of analysis (Sævik, 2017).

The static analysis consists of one analysis when the static configuration is reached and the route contact points are obtained. First step is the performing of S-lay screening. S-lay screening simulation implies simplified approach of pipeline feeding. This simulation is controlled by STATIC-SIMLA time control card and the analysis is performed by AUTOSTART control card. Next step is the performing S-lay feeding. This step is based on realistic approach. During simulation given configuration reflects a feed process, when the pipe gets fed out and the lay process is simulated. The static results are obtained after the performing of feeding analysis. The pipeline feeding is controlled through the STATIC-FEED time control card and the analysis is performed through the TIMEINIT control card, which is based on the AUTOSTART from the initial configuration. The difference from the S-lay screening analysis is that the actual lay process is simulated in the present analysis. The pipe elements experience the operation from being fed out from the lay vessel to resting on the seabed. Hence, history-dependent effects can be modelled, such as seabed friction and elastoplastic material behaviour (Sævik, 2017).
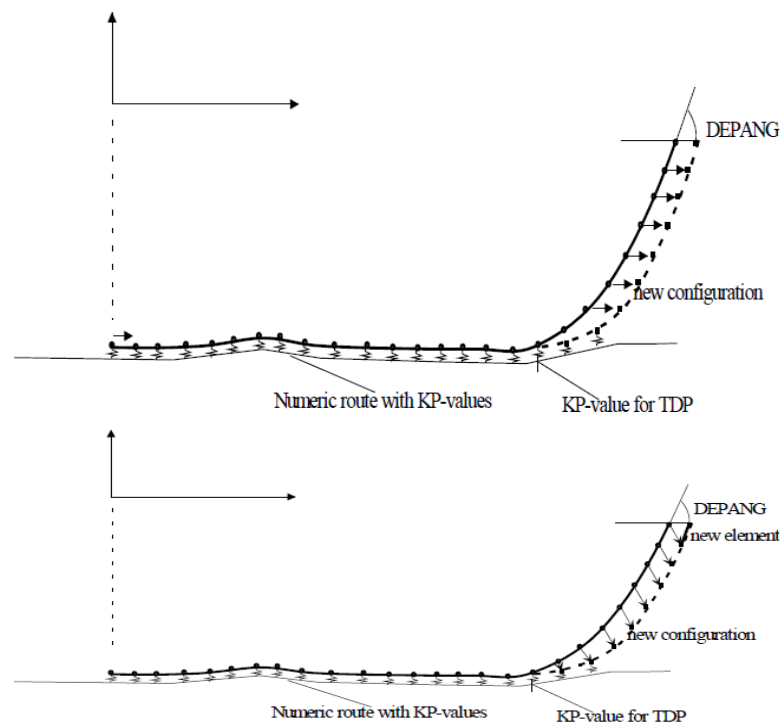
Figure 36 – Simplified and realistic approaches of S-lay process (Sævik, 2017)

The dynamic analysis is then performed in order to get the dynamic response taking into consideration environmental effects, namely waves and currents. The analysis is subjected to be implemented at the laying stage where the dynamic impact is high. As severe environmental conditions, the combination 10-year return condition for waves combined with the 100-year return condition for current was applied. The dynamic analysis is performed as a RESTART of the initial configuration in the control card.

When it comes to the input of natural conditions, a flat seabed with constant water depth of 80 is assumed. For wave modelling Jonswap spectrum was applied to describe an irregular sea state with duration of 10800 seconds. Current effects have been applied based on a 100-year extreme current, with the following current profile:

Table 17 – Current profile

Depth	100-year current [m/s]
0	1,57
20	1,15
40	0,78
80	0,56

The soil condition is taken as clay silt, and friction factor was taken during meeting with company employees. The friction factor of μ=0.35 is used in the SIMLA analysis in both lateral and axial direction. In SIMLA, the seabed has been modelled by means of the CONT125 contact element with transverse y-direction additional material curve in order to consider pipeline penetration. The contact interface between the pipeline and the seabed is determined by the CONTINT card. The contact force in the vertical direction is determined by linear stiff springs which are connected vertically to the pipe. This is implemented in SIMLA by defining a hyperelastic material behaviour with a force-displacement curve of constant slope. The material curves in the horizontal plane are defined by elastoplastic material behaviour with kinematic hardening (Sævik, 2017).

For post-processing the results, Simpost and Dynpost are utilized in order to extract the results from simulation file, and MatrixPlot is used to create plots.

For checking lateral on-bottom stability of curved laid pipeline axial force, moments and displacement of curved section have been estimated and studied.

The static analysis assumes that the pipeline is fed out from pipelaying vessel and laid along a predetermined route. Static simulation does not consider waves and current loads.

Figure 37 – Simulation process in SIMLA

After static analysis during predefined route curved pipeline section has some axial force, moments and displacement.
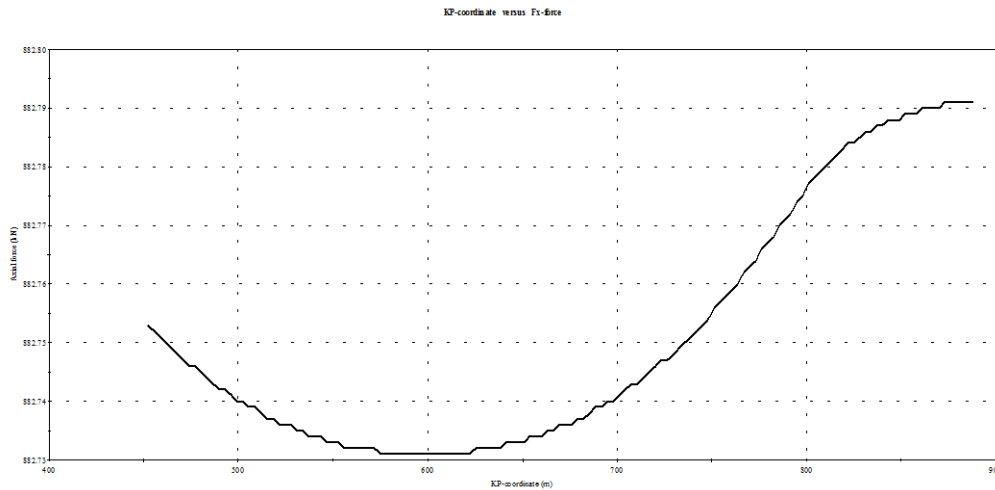

Figure 38 – Axial force in the pipeline

The above given graph shows the tension in curved pipeline section at the seabed. This plot represents the maximum tension in the pipeline during S-laying process. Given tension is provided by vessel tension capacity (6 MN) and does not exceed it.

Next important parameter is the moment along the curved section. Maximum moment must not exceed the allowable moment value. Allowable bending moment capacity can be calculated as:

$$M = Z * SMYS$$

In case of exceeding of allowable bending moment, pipeline can undergo plastic deformations and future moment increasing may lead to failure cause.
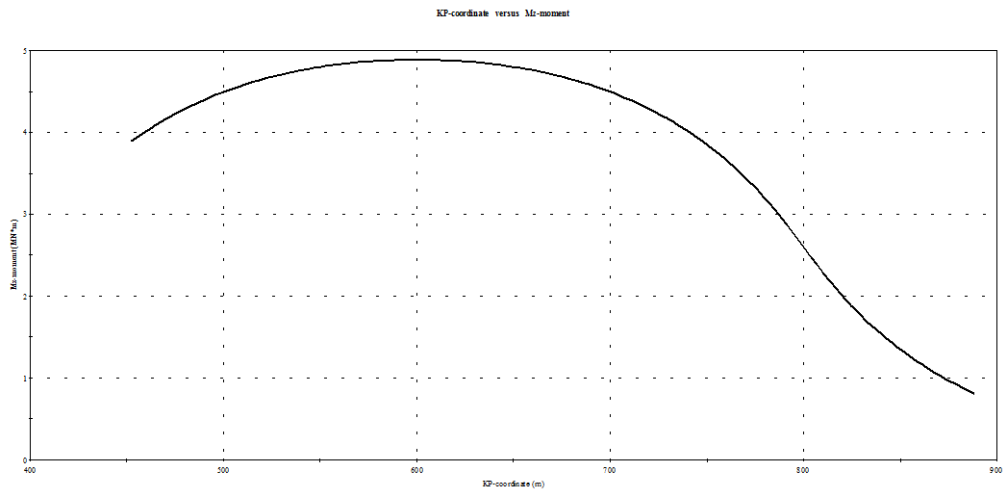
Figure 39 – Z-moment of the curved pipeline section

The displacement of curved pipeline has a significant meaning. In case of huge lateral displacements, turnpoints are necessary. For static simulation, waves and current loads were not taken into consideration. Pipeline has been penetrating into soil. Penetration depth influences passive resistance a lot, consequently passive resistance contributes to the restrictions of lateral displacements in robust manner.
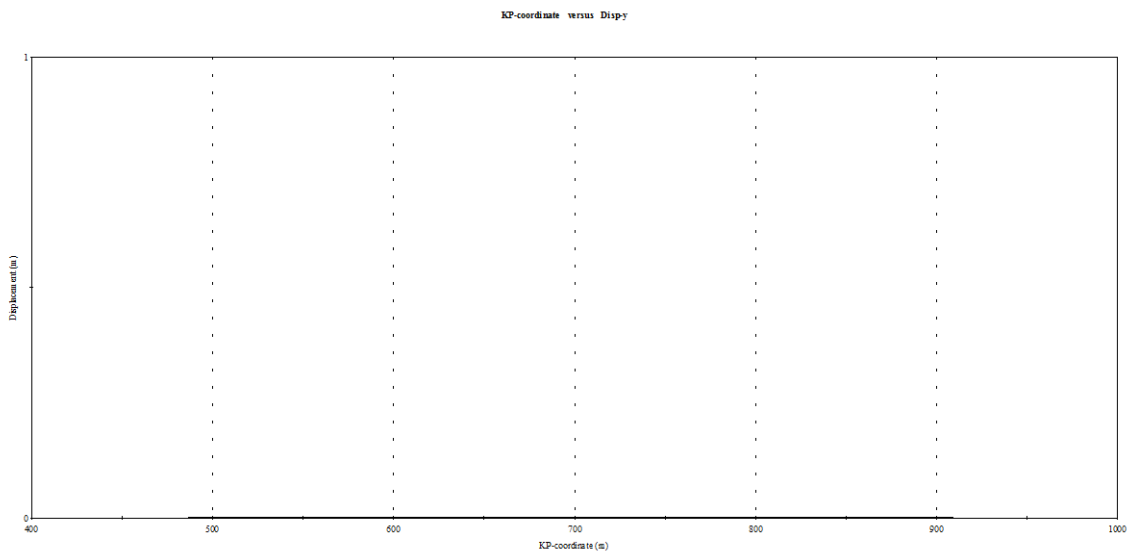
Figure 40 – Pipeline displacement is zero along y-axis

As it is shown in the figure, curved pipeline section does not undergo lateral displacements and stays fixed on the seabed. Passive resistance force affords to keep pipeline in stable manner without movements. Table 18 represents summary results for static process.

Table 18 – Total results of static analysis

Max. Axial force	Max. Moment	Max. Displacement
882,8 kN	4,8 MN*m	0 m

In dynamic analysis, a 3-hour sea state described by Jonswap spectrum with peak period 12.5 seconds and a significant wave height of 6.2 meters has been carried out. Due to the dynamic analysis is time-consuming enough, only one dynamic analysis with full sea state has been performed. In order to save time for simulations, short time interval was utilized. For other analyses, time interval of 300 seconds was taken. This was performed because the most dangerous response might occur at the same time interval during a sea state with the same seed value. In dynamic analysis pressure and gravity force are included immediately, whereas waves and current have introduced piecemeal. The results for full sea state and for 300-second time interval are nearly similar. The difference between them is quite slight. Thus, short time interval has been used as the representative of 3-hour sea state.

After the representation of full sea state, the results of dynamic analysis were provided. The outcomes of axial force for curved pipeline section during sea state are plotted in Figure 41.
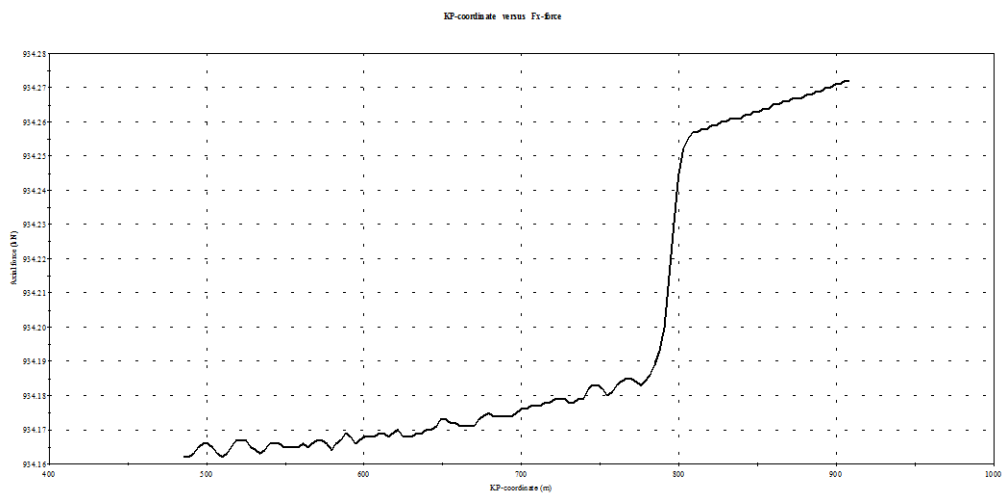
Figure 41 – Axial force in the pipeline

It is possible to see from the plot that there is the rising of tension in the pipeline, i.e. the pipeline gets stiffer. Compared to static analysis, the dynamic tension is higher due to movement resistance at touch-down area becomes bigger, consequently it is more difficult to pull out pipeline along curve section.

Moment obtained in dynamic analysis differs insignificantly compared to static analysis. The maximum value of moment does not exceed allowable value. The increasing of moment is associated with pipeline-seabed interaction. The outcomes in Figure 42 show the maximum moment during the full sea state.
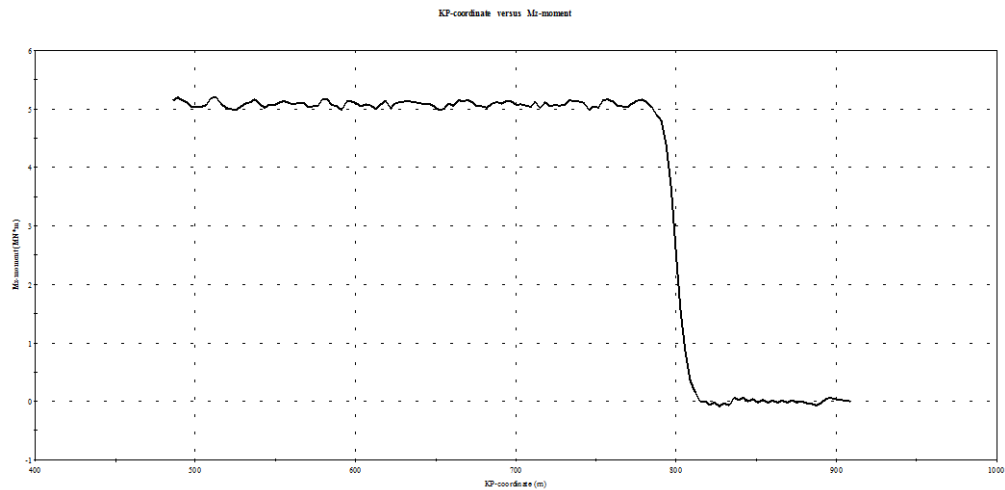
Figure 42 – Z-moment of curved pipeline section in dynamic analysis

In dynamic analysis, curved pipeline section gets lateral displacement. The pipeline obtains movements due to waves and currents load. Figure 43 shows results.
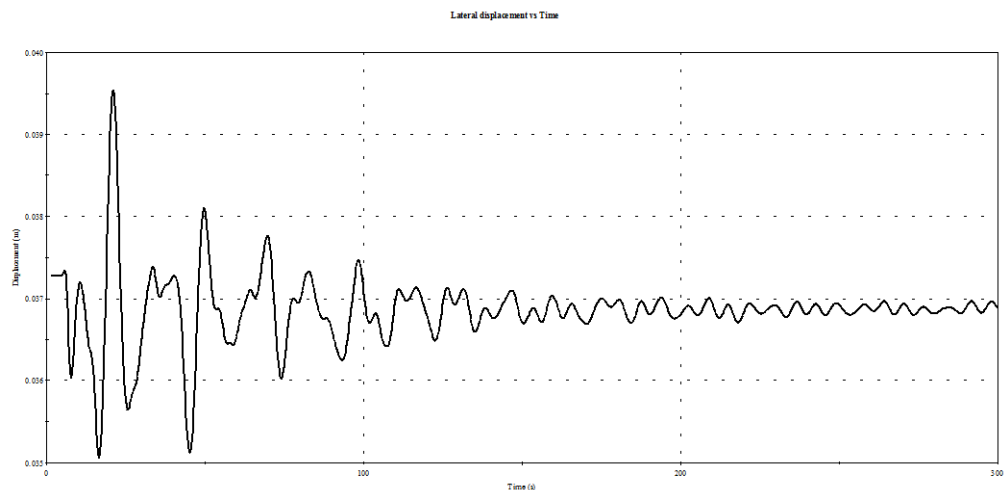

Figure 43 – Lateral displacement of curved section in dynamic analysis

As it can be seen, that curved pipeline gets maximum displacements in range from zero to 100 seconds. Since pipeline has some penetration depth, passive force prevents further displacements of pipe. Waves and currents make the pipeline fluctuate. However, seabed soil restricts significant movements and slippage. Table 19 gives total outcome for dynamic analysis.

Table 19 – Total outcomes for dynamic analysis

Max. Axial force	Max. Moment	Max. Displacement
934,3 kN	5,1 MN*m	0.04 m

As it was mentioned earlier, natural seabed obstacles and possible subsea infrastructure along route can claim the curved sections of pipeline. Along pipeline route in limited areas, there can be present several horizontal curved sections. In accordance with (DNV, 2010) sufficient soil

resistance can keep pipeline in laid manner, avoiding slippage or straightening. One crucial component is passive force, which influences the lateral displacement of pipeline. If the soil friction is not sufficient, it may be necessary to introduce turnpoints to support the pipeline.

For above investigated case, soil resistance is rather high and pipeline undergoes small lateral displacements, which can be omitted, consequently there is no reason to establish turnpoints. However, there are possible areas with low passive resistance along pipeline route. In order to avoid slippage and to ensure lateral stability, defined number of turnpoints is necessary.

For the calculation of required turnpoint number, non-FEA methodology was applied. The methodology considers next statements:

- Pipe bending moment due to initial curvature;
- Pipe bending moment due to positioning tolerance based on simplified beam theory;
- Pipe bending moment on turnpoint due to pipeline tension;
- Utilization factor which is present as ratio of moments and appears peculiar safety criteria;
- Curved arc length between turnpoints.

The force, which interacts with a turnpoint, is calculated proposing that the force is "smudged" over the arc length. The pipeline involves contact with all turnpoints. Taking into consideration constant bottom tension and uniform soil resistance, the impact to each turnpoint is identic. After the calculation of necessary distance between turnpoints, it is possible to find their number for the holding of pipeline in curved position. Assuming only initial penetration of pipeline and less passive resistance force, the number of turnpoints is calculated below. Table 20 represents initial data for calculation.

Table 20– Initial data

Parameter	Value
Elastic sectional modulus of pipe, Z	0,0168 m^3
Passive soil resistance, F_R	0,1 kN/m
Maximum dynamic bottom tension, T_b	934 kN
Distance between turnpoints, L	[1, 350] m
Positioning tolerance, δ	0,3 m
Curve radius, R	350 m
Length of curved section, L1	400 m

There are next steps to calculate the number of turnpoints. Detailed calculation is present

in Appendix A.

1. Find required friction force and load at turnpoint;
2. Calculate moment due to initial curvature, moment due to positioning tolerance, moment due to pipeline tension;
3. Calculate utilization ratio;
4. Make a plot of utilization factors;
5. Calculate arc length, load at turnpoint and the number of turnpoints.

The outcomes are present in Table 21.

Table 21 – Turnpoint calculation results

Parameter	Value
Arc length, s	40,02 m
Load at turnpoint, F_{TP}	87,5 kN
Number of turnpoints, n	10

Chapter 4. Technological and economic evaluation of facilities

Having discussed the choice of platform and the features of pipeline design/installation, it is necessary to take into consideration technological readiness of given assets and to show possible risks during Pobeda field lifecycle.

Technology readiness level is a way of evaluation technology maturity of new technology or product (Wikipedia, 2019). This approach is based on API document (API, 2017) and is applied in petroleum industry. Technology readiness level has a scale with numbers from zero to seven. Each number gives information about the maturity of chosen technology. The Table 22 gives a description of levels.

Table 22 – Technology readiness level

Technology readiness level (TRL)	Description
TRL 0	Unproven idea. No testing was implemented
TRL 1	Concept demonstrated. Basics of technology was demonstrated; some features are clarified.
TRL 2	Concept validated. Model works in laboratory conditions. Need specified improvements.
TRL 3	New technology tested. Technology works in limited range of operating conditions.
TRL 4	Technology qualified for first use. Technology tested in intended environment, simulated or actual.
TRL 5	Technology integration tested. Full-scale prototype built and integrated into operating system (functionality tests)
TRL 6	Technology installed. Technology shows acceptable performance and robust during period.
TRL 7	Proven technology. Technology operates successfully in actual conditions.

In accordance with Table 22, there are next technology readiness levels of platform concept and pipeline transportation system in Kara Sea conditions.

Offshore construction. The technology readiness levels of offshore platform for drilling and production of hydrocarbon resources is below:

- Design and construction of GBS: TRL=7;
- Transportation and installation of GBS: TRL=6;
- Working crew delivery to the platform: TRL=6;
- Coupling GBS with SPS as possible variant: TRL=6;
- Stable operating state of GBS under harsh conditions under lifecycle: TRL=4;
- Autonomous work of GBS during long period time: TRL=5;
- Support and IMR strategy: TRL=3.

For improved platform operation and protection from hazards of environment, it is possible to apply active ice protection, ice management and smart technologies (IoT, digitalization).

Pipeline transportation system. The evaluated technology readiness levels of the elements of the pipeline transportation system are present below:

- Design and fabrication of pipeline: TRL=7;
- Installation of pipeline (curved sections, short "operational window"): TRL=5;
- Operation of pipeline: TRL = 5;
- Trenching of pipeline at near-platform and coastal zones: TRL = 4.

The installation and operation of the subsea pipeline requires accurate detailed analyses for the development of Pobeda field. The aim of master thesis was to show the robust on-bottom stability of curved laid sectors for avoiding natural seabed obstacles and private territories. However, there may require new technologies for robust pipeline operation. The main aspects about proper pipeline system are:

- Presence of ice-resistant vessels and pipelaying operations in ice-free period;
- Robust pipeline inspection during whole lifecycle;
- Detailed discussions and analysis about trenching aspect and flow assurance.

Besides technological readiness of technology, risk analysis is crucial aspect during field development too. Moreover, the Arctic nature is very sensitive and it is necessary to perform any operations without global hazardous consequences.

The next risk matrix provides possible risks and risk reduction factors. Risk matrix has three criteria for two types of infrastructure. Table 23 is present below.

Table 23 – The matrix of risks for Pobeda field assets due to natural and climatic conditions

Risk factors and negative impacts caused by climatic risks risk reduction	Risk reduction factors	Probability	The magnitude of the effect	Controllability	Probability	The magnitude of the effect	Controllability
		Offshore ice-resistant fixed platform (OIRFP)			Subsea gas pipeline from platform to BCS in the area Harasavey		
Damage to the structures of platform, supply vessels, tankers due to extremely strong ice load	• The reliable ice-resistant design of the support base of the MLSP was chosen. • Carrying out tests on the stability of the platform to wind, wave, ice loads. • Ice management • Regulation of ice conditions and reduction of ice load on the OLS • Maintaining the required ice conditions in the port area;	yellow	yellow	yellow	-	-	-
Damage ice formations (icebergs, stamukha) located on the bottom or buried in the ground underwater pipelines, cables	• Vessels used in the exploration, have to crack the ice formation or to change the course of icebergs. • Conduct comprehensive monitoring of ice conditions in the mining areas and transport routes; the provision of quality satellite data plots, towing and deflection of icebergs in the simultaneous presence of icebergs and ice fields. • Introduction of limit values of characteristics of ice conditions for technological and service operations (drilling, approach of vessels, acceptance/transfer of cargo, lifting operations, landing / disembarkation of people, etc.).	-	-	-	green	red	red
Icing-up of structural elements of the upper structure of the platform	• The main working areas are closed and have temperature and ventilation control. • The equipment is located in the open air, equipped with protection against icing-up and low temperatures.	red	green	yellow	-	-	-
Permafrost melting, loss of soil bearing capacity	• Using the method of pile construction with thermal stabilization of the soil around each support pile. • Monitoring of soil condition in the locations of objects.	yellow	red	yellow	yellow	red	yellow

Table 23 continued

Risk factors and negative impacts caused by climatic risks risk reduction	Risk reduction factors	Probability	The magnitude of the effect	Controllability	Probability	The magnitude of the effect	Controllability
		Offshore ice-resistant fixed platform (OIRFP)			Subsea gas pipeline from platform to BCS in the area Harasavey		
Structural damage due to a strong earthquake	• Relatively low seismicity of the development region (5-point earthquake no more than 1 time per 100 years). • The robust design of the support base has been selected. • The pipeline system is designed to be resistant to possible seismic loads.	🟢	🟡	🟢	🟢	🟡	🟡
Structural damage due to severe storm (extreme waves and wind)	• The robust design of the support base has been selected. • Carrying out tests on the stability of the platform to wind, wave, ice loads.	🟡	🟢	🟢	🟢	🟢	🟢
Complexity of oil spill response and personnel evacuation in ice conditions	• Create a disaster recovery items and specialized disaster recovery services. • Application of special oil-gathering equipment for oil spill response in ice conditions. • Application of a special system for emergency evacuation of personnel from the platform to the ice.	🟡	🟡	🟡	-	-	-
Breakage of lifting equipment due to bad weather conditions (extreme wind, blizzard)	• Compliance with the rules and regulations for the safe operation of lifting equipment. • Accounting for weather conditions in the operation of lifting equipment. • Use of wind measurement devices and wind maps.	🔴	🟢	🟢	-	-	-
🟢 Low 🟡 Medium 🔴 High							

Besides technological readiness in severe environment, Arctic field development requires significant investments and expenditures, which depend on the total effect of environmental and technological conditions. This chapter includes the prices of two objects, namely GBS structure and pipeline from Pobeda field to onshore facility.

GBS structure

Offshore construction comprises two parts: topside and support block. Platform topside contains next systems and complexes:

- Accommodation block;
- Helideck;
- Drilling facilities;
- Processing complex;
- Power complex;
- Utility systems;
- Control system;
- Navigation system;
- Communication system;
- Others.

Considering the above complexes and systems, during the conversation with Rosneft Company employees the average weight of topside is 46000 tons. For the evaluation of topside cost next formula is taken into account:

$$C = W * c, where\ c\ is\ specific\ cost\ taken\ as\ average\ value\ of\ project$$

$$- analogues\ by\ Rosneft\ company\ \left(\frac{bn\$}{ton}\right); W\ is\ topside\ weight.$$

$$C = 46000 * 0,000068 = 3,1\ billion\ \$$$

The reinforced concrete support block of GBS structure is taken 344595 tons as analogue of Hibernia support block with consideration of water depth (the height of Pobeda support block equals 85 meters, while Hibernia support block height is 111 meters). In accordance with various economic assessments conducted for the company Rosneft, the specific cost of reinforced concrete (bn $/ton) is taken 0,0000039.

$$C = W * c = 344595 * 0,0000039 = 1,3\ billion\ \$$$

Pipeline

For pipeline cost evaluation, two main costs are taken into account, namely pipeline manufacturing expenditures and pipeline installation cost. Necessary data was taken from Subsea 7 Company.

- Pipeline manufacturing expenditures: pipe 1020x22 mm for 1 meter - 3600,3$; concrete coating (60mm) and anticorrosion coating (4mm) for 1 meter - 1400,7$.
- Overall pipeline installation cost (vessel rent, crew salary and etc.) - 137221,3$/day

Assume that pipelaying rate is 7 km/day. Thus, it takes 93 days to install pipeline from Pobeda field to onshore facilities. Table 24 gives information about overall expenditures.

Table 24 – Overall costs associated with pipeline route 4

Pipeline manufacturing expenditures	Overall pipeline installation cost	Sum
3250,7 million $	12,8 million $	3263,5 million $

In case of an actual development, a route optimization study must take place where the costs of the pipeline material and installation for different routings must be compared to the costs of trenching parts of the pipeline. We have discussed routing number 4 (Figure 28) as this route will require the least distance of trenching. In this respect also the *feasibility* of trenching the pipeline to required depth in potentially soft soils must be considered.

Chapter 5. Conclusion and future recommendations

Arctic shelf has huge resource potential and it should be developed in future, despite severe conditions. Some conclusions are present below:

1. Icebergs represent great danger during the arrangement of Pobeda field. Ice management and iceberg movement forecasting are of great practical importance. To monitor the spread of icebergs and their drift, satellite monitoring, aerial photography from a helicopter or an unmanned aerial vehicle are utilized. The possibility of the iceberg appearance practically throughout the entire water area of the Kara Sea indicates a real danger to the offshore structures, subsea facility and submarine pipelines. It is vital to organize complex engineering surveys before field development. Subsea facilities must be located below the keel of drifting icebergs or be trenched to a depth where the icebergs will not influence.

2. An offshore ice-resistant fixed platform is a large engineering structure. The conditions for the design and operation of such facilities impose specific requirements. The arctic regions are characterized by a high content of oxygen in the water and low air temperatures. The behavior of reinforced concrete in such conditions is more favorable than steel, the cost of reinforced concrete is significantly less than the cost of special steels. Moreover, the platform of Hibernia project is a robust example for seas with iceberg presence, consequently a similar structure can be used for Pobeda field.

3. Subsea pipeline route was chosen to avoid grounded icebergs and drift icebergs with maximum drift. The selected route includes curved pipeline sections, which are considered to be stable due to high passive resistance force of the soil. It was done simulation only for the one worst case in Kara Sea conditions. As for future recommendation, different cases should be investigated. Various wave directions and penetration depth should be considered in future analysis. Pipe-soil interaction should be researched in order to get more accurate seabed friction value and penetration depth. If there is insufficient soil resistance turnpoint position and their tolerance should be investigated for each case.

In conclusion, it is necessary to note that existing technologies do not fulfill all requirements to ensure safe and reliable Pobeda field development. New approaches and technologies should be designed, tested and applied. In accordance with (Zolotukhin, 2019), the exploitation of Pobeda field will start no sooner than in year 2030.

References

AARI, Long-term forecast of Kara sea natural conditions-South-Western part (2006). Internet portal. http://www.aari.ru/resources/f0018/2013/lo_SW_kara.html, In Russian.

AARI, The natural conditions of Kara Sea (2017). Internet source, http://www.aari.ru/resources/a0013_17/kara/Atlas_Kara_Sea_Winter/text/rejim.htm , In Russian.

All patents. (2015). Internet source. http://allpatents.ru/patent/2421572.html, In Russian.

API Specification 5L (2000). Specification for Line Pipeline. 42nd edition, Washington D.C., USA.

API (2017). API RP 17N. Recommended Practice on Subsea Production System Reliability, Technical Risk, and Integrity Management. American Petroleum Institute, the USA.

Arctic atlas. Bathymetry of Barents and Kara seas (2001). Internet source. http://research.bpcrc.osu.edu/foram/maps.htm

Bai, Y. (2001). Pipeline and Risers. Elsevier, Kidlington, Oxford. UK.

Bai Y., Bai Q. (2005). Subsea Pipelines and Risers. Elsevier, Oxford, UK.

Bassem Y., Dermot O. (2017). On-bottom stability analysis of submarine pipelines, umbilicals and cables using 3D dynamic modelling. OTC-27727-MS. Offshore Technology Conference in Houston, USA.

Borodavkin P.P. (2006). Offshore oil and gas facilities. Part 1. Textbook for universities. NEDRA, Moscow.

DNV (2017). DNV-RP-F114. Pipe-soil interaction for submarine pipelines. Det Norske Veritas, Høvik.

DNV (2012). DNV-OS-F101. Offshore Standard for Submarine Pipeline Systems. Det Norske Veritas, Høvik.

DNV (2010). DNV-RP-F109. On-Bottom Stability Design of Submarine Pipelines. Det Norske Veritas, Høvik.

DNV (2007). DNV-RP-F110. Global Buckling of Submarine Pipelines. Det Norske Veritas, Høvik.

Eie R., Rognaas G. (2014). Fixed platforms – Development challenges in ice infested Arctic. OTC 24578. Technology conference in Houston, USA.

Gabdullin I. (2014). Technical-economic justification of Pobeda field development. Report. (Private communication from Rosneft, Moscow)

Galimov E., Kodina L., Stepanets O., Korobeinik G. (2006). Biogeochemistry of the Russian Arctic. Kara Sea: Research results under the SIRRO Project, 1995–2003. Russian Academy of Sciences, Moscow, Russia.

Geography, Temperature and salinity of Russian Arctic seas. Internet portal.

https://geographyofrussia.com/temperatura-solenost-plotnost-vody-morej-rossijskogo-sektora-arktiki/, In Russian.

Heinkel. J. (1997). Oil and Gas resources of the West Siberian Basin, Russia. Energy Information Administration Office of Oil and Gas, U. S. Department of Energy. http://webapp1.dlib.indiana.edu/virtual_disk_library/index.cgi/4265704/FID1578/pdf/oil/061797.pdf

Huaiyin L., Xuebo D., Kai Z. (2015). Review and outlook on Arctic Offshore facilities and Technologies. OTC-25541-MS. Conference in Copenhagen, Denmark.

ISO (2010). ISO 19906. Arctic Offshore Structures. International Standardization Organization, Geneva, Switzerland.

Jaeyoung L. (2007). Introduction to pipelines and risers. http://www.jylpipeline.com/Pipeline_2009C_Brief.pdf

Karunakaran D. (2018). Pipelines and Risers lecture notes. UiS, Stavanger, Norway.

Keghouche I. (2010). Modelling the dynamic and drift of icebergs in the Barents Sea. PhD dissertation. University of Bergen, Norway.

Kyriakides S., Corona E. (2007). Mechanics of Offshore Pipelines Volume 1. Elsevier, Oxford. UK.

Løset, S., Shkhinek K., Gudmestad O., and Høyland, K. V. (2006). Actions from Ice on Arctic Offshore and Coastal Structures: Student's Book for Institutes of Higher Education. Publisher "LAN", St. Petersburg, Russia.

Matskevitch D.G. (2006). Technologies for Arctic offshore exploration and development. SPE 102441. Conference in Moscow, Russia.

Palmer A., King R. (2008). Subsea Pipeline Engineering. 2d edition, PennWell, Tulsa, Oklahoma, USA.

Perinet D., Frazer I. (2007). J-Lay and Steep S-Lay Complementary Tools for Ultradeep Water. OTC Paper 18669-MS. Offshore Technology Conference, Houston, USA.

Rosneft, Rosneft's experience marine operations in Arctic (2017). Presentation for network meeting (Private communication).

SP (2012). SP 38.13330.2012. Loads and actions on hydraulic engineering constructions (wave and ice generated and from ships). Minregion of Russia, Moscow, Russia.

Spiridonov A., Gavrilo M, Krasnova E. (2011). Atlas of marine and coastal biological diversity of the Russian Arctic. WWF Moscow, Russia. https://wwf.ru/en/resources/publications/booklets/atlas-of-marine-and-coastal-biological-diversity-of-the-russian-arctic/

Stantec (2013). Hibernia Oil and Gas Production and Development Drilling Project

Environmental Effects Monitoring Plan. https://www.cnlopb.ca/wp-content/uploads/eem/eem_2013_1_hdmc.pdf

Sævik S. (2017). SIMLA – User guide. MARINTEK, Trondheim, Norway.

Sævik S. (2008). SIMLA - Theory Manual. MARINTEK, Trondheim, Norway.

Tewolde A. A. (2017). Pipelay with residual curvature. Master Thesis, UiS, Stavanger, Norway.

Wikipedia. (2019). Technology readiness level definition. https://en.wikipedia.org/wiki/Technology_readiness_level

White D., Cluckey E., Randolph M., Boylan N., Bransby M., Fugro A., Zakeri A., Hill A., Jaeck C. (2017). The state of knowledge of pipe-soil interaction for on-bottom pipeline design. OTC-27623-MS. Offshore Technology Conference in Houston, USA.

Xu P., Gong F. S., Zhang Y., Chen C. (2018). Parametric Study on Dynamic Tension Behavior of Offshore Pipeline for Deepwater S-lay Operation. Conference ICEMEE 2018, China. https://www.researchgate.net/publication/325567438_Parametric_Study_on_Dynamic_Tension_Behaviour_of_Offshore_Pipeline_for_Deepwater_S-lay_Operation

Zolotukhin, A. (2019). Arctic technology courses lecture notes. UNIS.

Appendixes

Appendix A. Turnpoint calculation, MATLAB 2016.

```
E=207000000000; % Young's modulus, Pa
Length=400;     % Curved part length, m
Do=1.020;       % Outer diameter, m
t=0.022;        % Wall thickness, m
Ws=1.083;       % Submerged weight, kN/m
SMYS=414000000; % SMYS, Pa
R=350;          % Curved radius, m
nu=0.35;        % Soil friction
T=934;          % Maximum dynamic bottom tension,kN
delta=0.3;      % Turnpoint tolerance, m
Fr=0.1;         % Passive resistance, kN
Di=Do-2*t;      % Inner diameter, m
I=pi/64*(Do^4-Di^4); % Moment of inertia, mm4
Z=2*I/Do;       % Elastic sectional modulus of pipe, mm3
M=SMYS*Z/1000; % Bending moment capacity, kN*m
Wer=T/R;        % Required friction force, kN/m
for i=1:350;
Ftp(i,1)=max((Wer-Ws*nu-Fr)*i);% Load at turn point, kN
end
```

```matlab
Mcur=E*I/R/1000; % Pipe Bending Moment Due To Initial Curvature, kN*m
for i=1:350;
Mtol(i,1)=(delta*16*E*I/((2*i)^2))/1000; % Pipe Bending Moment Due To Positioning Tolerance, kN*m
end
for i=1:350;
   x1(i,1)=R-((R^2-(i/2)^2)^0.5); % Moment arm, m
end
 Mpull1=(T-((nu*Ws+Fr)*R))*x1; % Moment due to Pull (tension), kN*m
 for i=1:350;
    x2(i,1)=R-((R^2-i^2)^0.5); % Moment arm, m
 end
 Mpull2=(T-((nu*Ws+Fr)*R))*x2; % Moment due to Pull (tension), kN*m
 UT1=(Mcur+Mtol+Mpull1)/M; % Utilization factor (Pipe is pulled to all turn points)
 UT2=(Mcur+Mpull2)/M;     % Utilization factor (Pipe skips one turn point)
 UTL=1;              % Limit
 for i=1:350;
    L(i,1)=i;
 end
 plot(L,UT1,L,UT2,L,UTL);
 Ls=40;                 % Selected length from graph
 fi= asin(Ls/(2*R));    % Intended angle, rad
```

```matlab
s=2*R*fi;                % Arc length, m
n_turn=Length/Ls;    % Number of turnpoints
```